Atmospheric Phase Correction

9th IRAM Millimeter Interferometry School
Grenoble, October 10-14, 2016

Michael Bremer

- Atmospheric phase fluctuations
  First encounters – the physics behind the scenes – turbulent times
- Monitoring
  What tool, please? – where to look – practical implementation
- Appearance in the Plateau de Bure data reduction
  Press the button, and smile – some useful checks – fine tuning

First encounters with atm. phase fluctuations

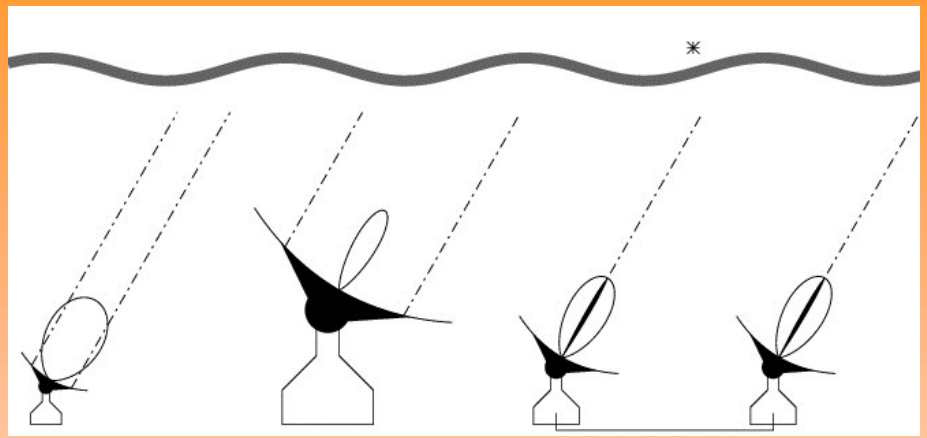

30m pointing under anomalous refraction

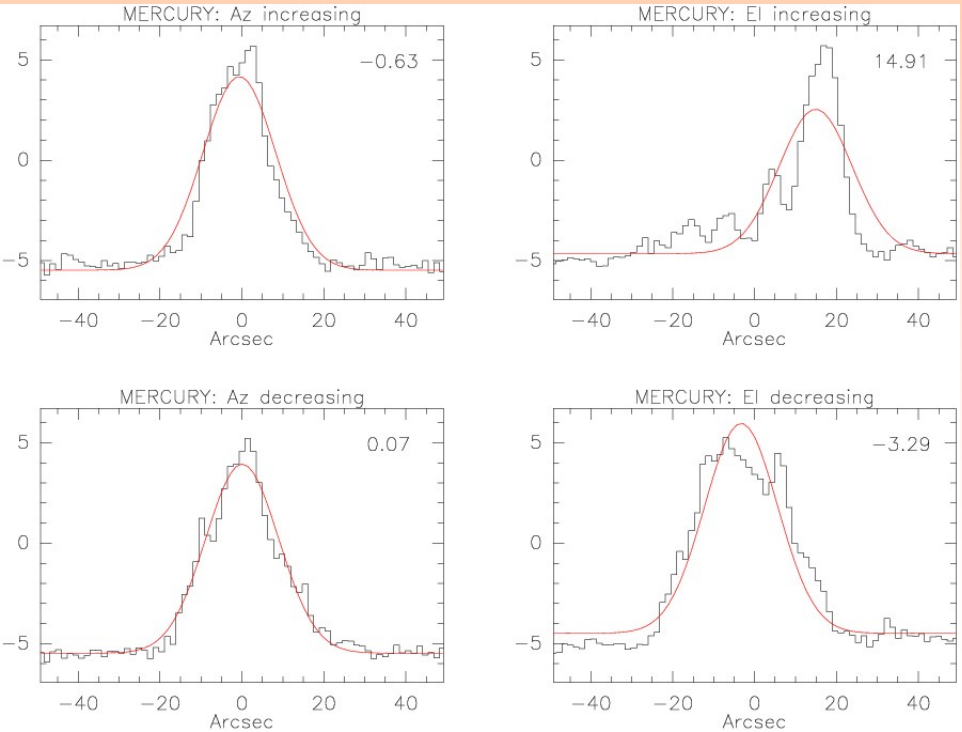

PdBI observation with phase noise

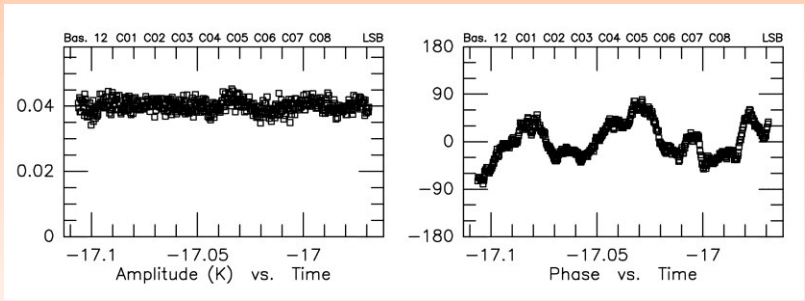

We will look at the PdBI phase noise in more detail …

First encounters with atm. phase fluctuations

6-antenna observation (15 baselines) in extended configuration, ~ 8 minutes

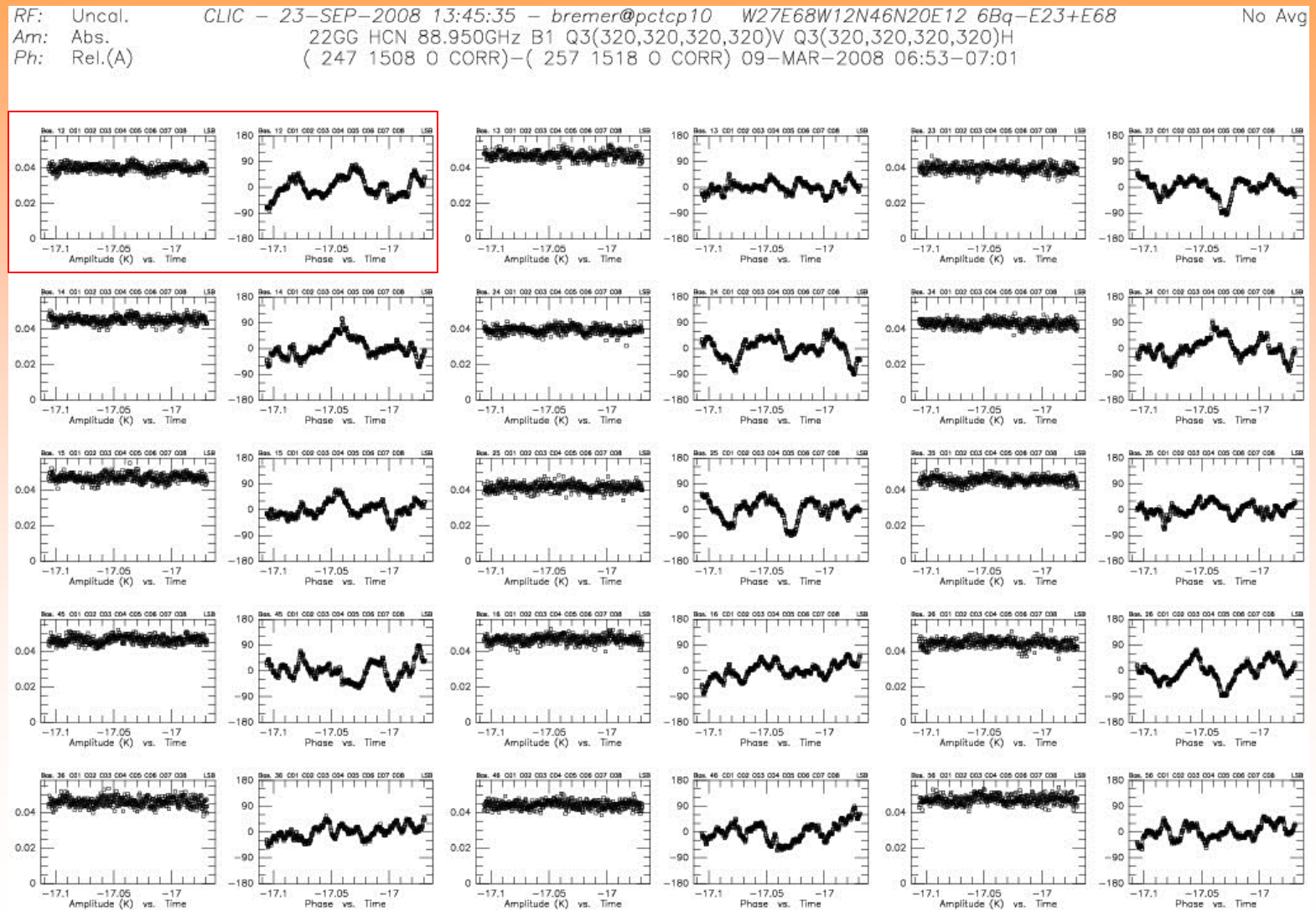

First encounters with atm. phase fluctuations

Three impacts on observations: a) the point source appears to move,

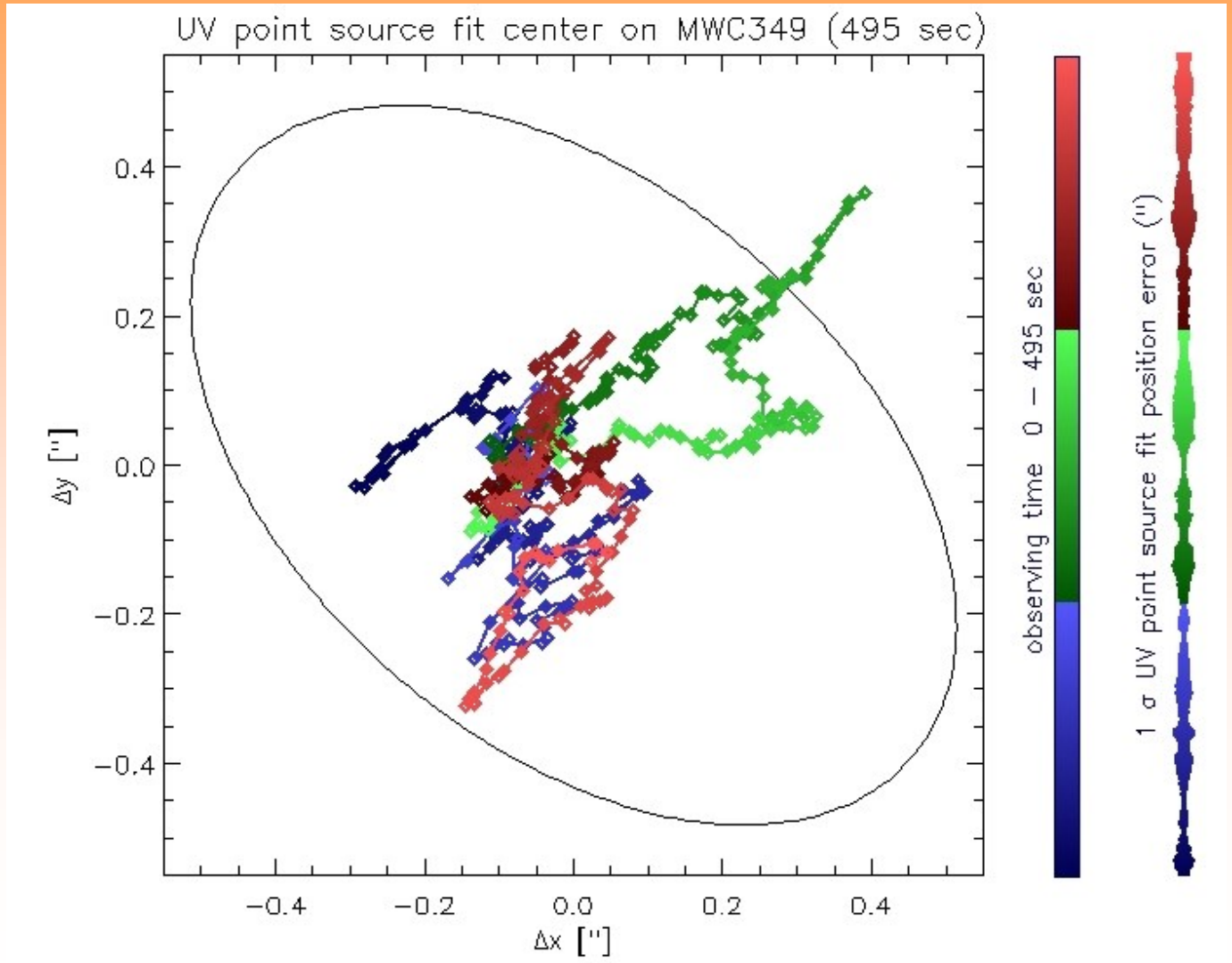

First encounters with atm. phase fluctuations

b) we loose integrated flux because visibility vectors partly cancel out. Formula:

$V_{OBS}=V_{IDEAL} \cdot \exp(-\varphi^2/2)$ with phase noise φ in radian.

Observations were at 89 GHz and average phase noise 30º: 12.5% loss.

If we would have used a frequency 2 or 3 times higher: 42% or 71% loss …

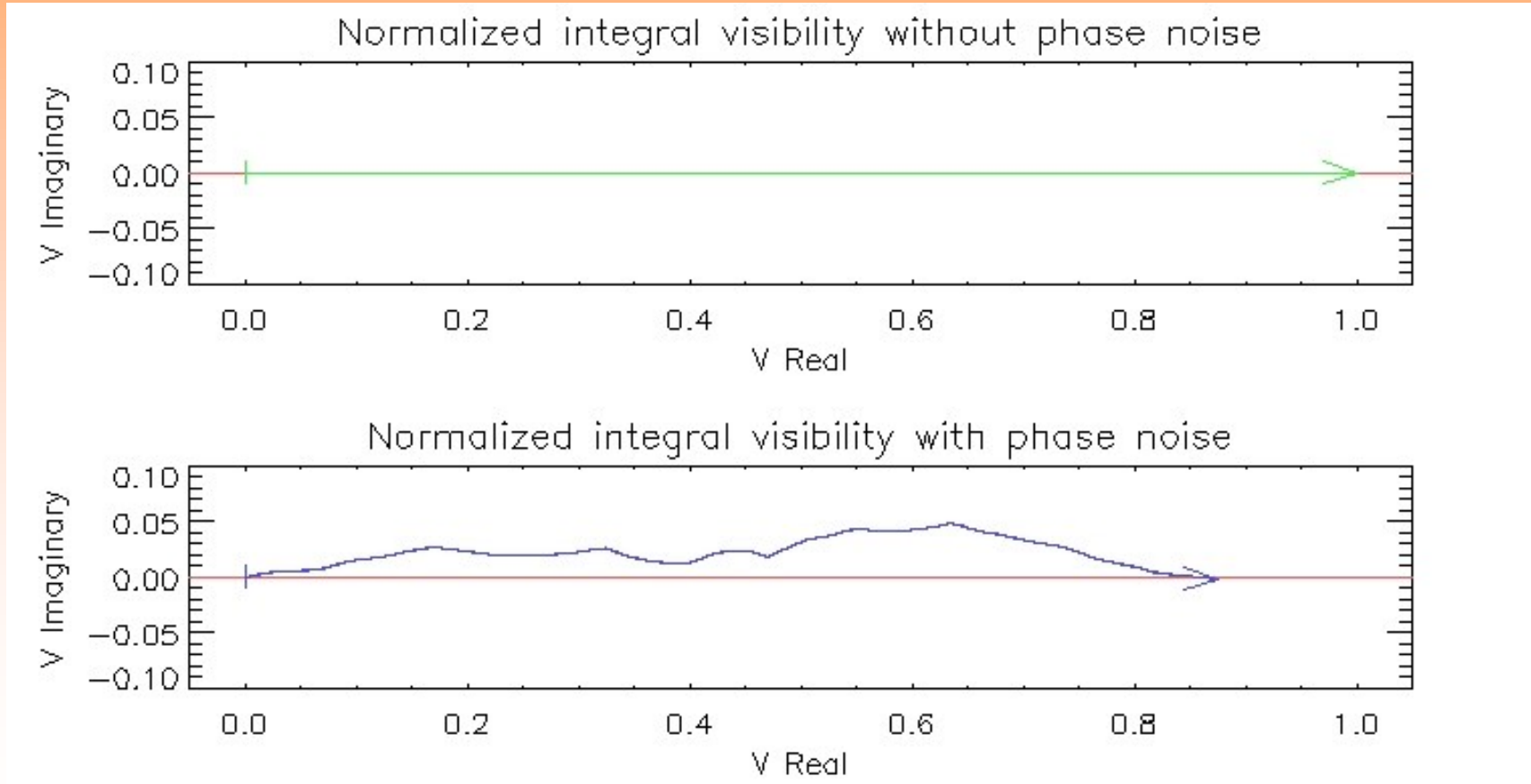

First encounters with atm. phase fluctuations

c) and we loose more signal on the longest baselines, which provide the finest details of our maps.

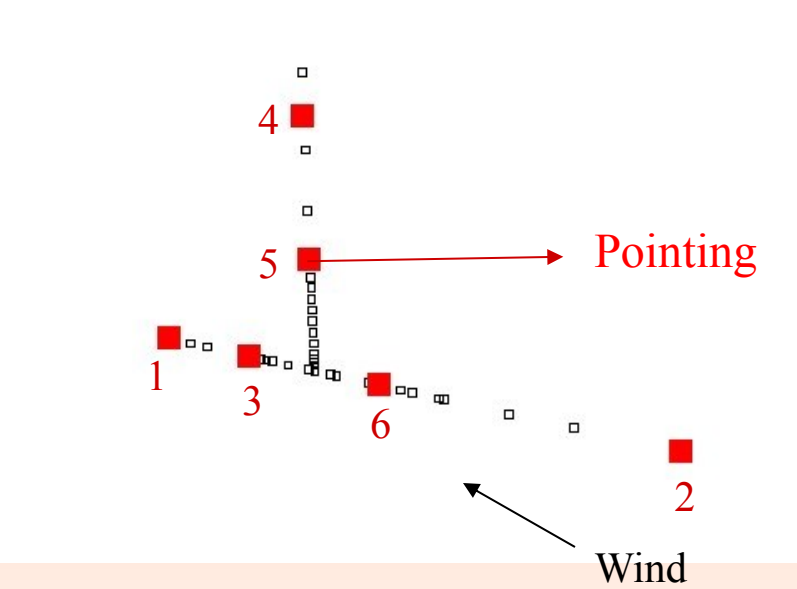

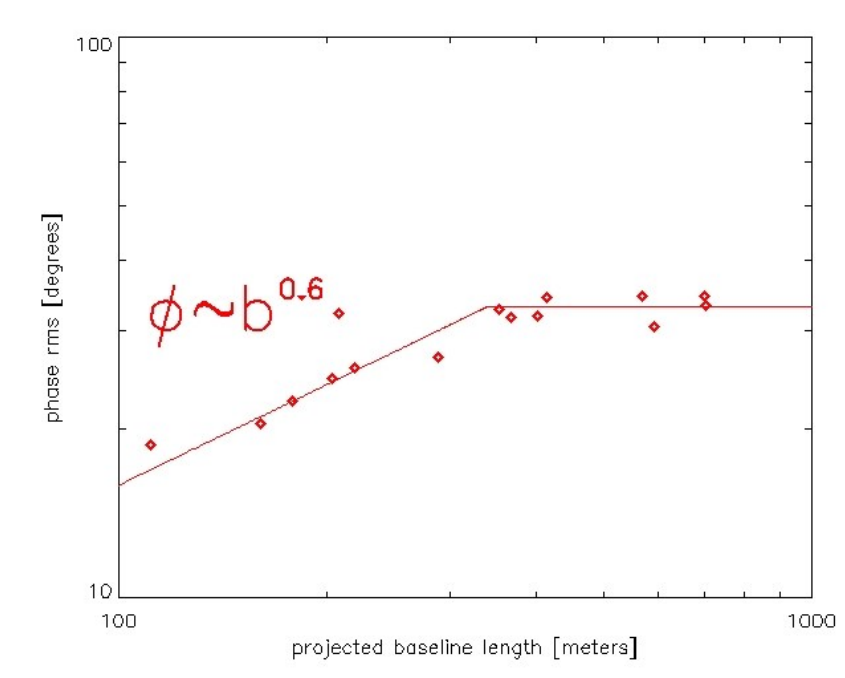

Configuration: W27-E68-W12-N46-N20-E12

Wind speed : 9 m/s from Azimuth -59°
Pointing : Azimuth=-91°, Elevation=67.3°
Frequency : 88.950 GHz

- *Atmospheric phase noise is worst on the longest baselines.*
- *The power-law break is weather dependent, and can be at several km.*

The physics behind the scenes

What we experience in the radio range differs from optical seeing.

Table 1: Expected image patterns for different scales of moist air turbulence.

Scale of turbulence:	FINE SCALE (diffractive regime, $a \ll D$)		INTERMEDIATE $a \leq D$	LARGE SCALE (refractive regime, $a > D$)
Phase variation over scale a:	$\Delta\phi < 1$ radian	$\Delta\phi > 2.6$ radians	$\Delta\phi > 2.5$ radians	
	VLBI		***Optical***	***30M, PDBI***
Short integration result	IMAGES superimposed on "error" beam	BLUR ("seeing disk")	SPECKLES	IMAGE MOTION (= Anomalous Refraction)
Remark	Images can still be formed. Some of the power is scattered to large angles (λ/a).	The diffraction limited beam disappears into the "error" pattern.	$(D/r_o)^2$ images	
Long integration result	same as snapshot result.	same as snapshot result.	BLUR (beam size convolved with seeing disk)	BLUR (In long integrations, the radio seeing disk is the smoothed envelope of the image motion.)
Point source image size:				
snapshot:	$\frac{\lambda}{D}$	$\frac{\lambda}{a}$	$\frac{\lambda}{D}$	$\frac{\lambda}{D}$
Long integration:	same	same	$\left(\frac{\lambda^2}{r_o{}^2} + \frac{\lambda^2}{D^2}\right)^{1/2}$	$\left(1.4\frac{\lambda^2}{r_o{}^2} + \frac{\lambda^2}{D^2}\right)^{1/2}$

Symbols: a = scale size of moist air packet; D = size of antenna, or interferometer baseline; r_o = diameter of atmospheric coherence region; at radius $r_o/2$, wavefront phase error $\Delta\phi = 2.6$ radians.

From: Downes and Altenhoff (1989), Anomalous Refraction at Radio Wavelengths, Proc. of the URSI/IAU Symposium on Radioastronomical Seeing, Beijing 15-19 May 1989

The physics behind the scenes

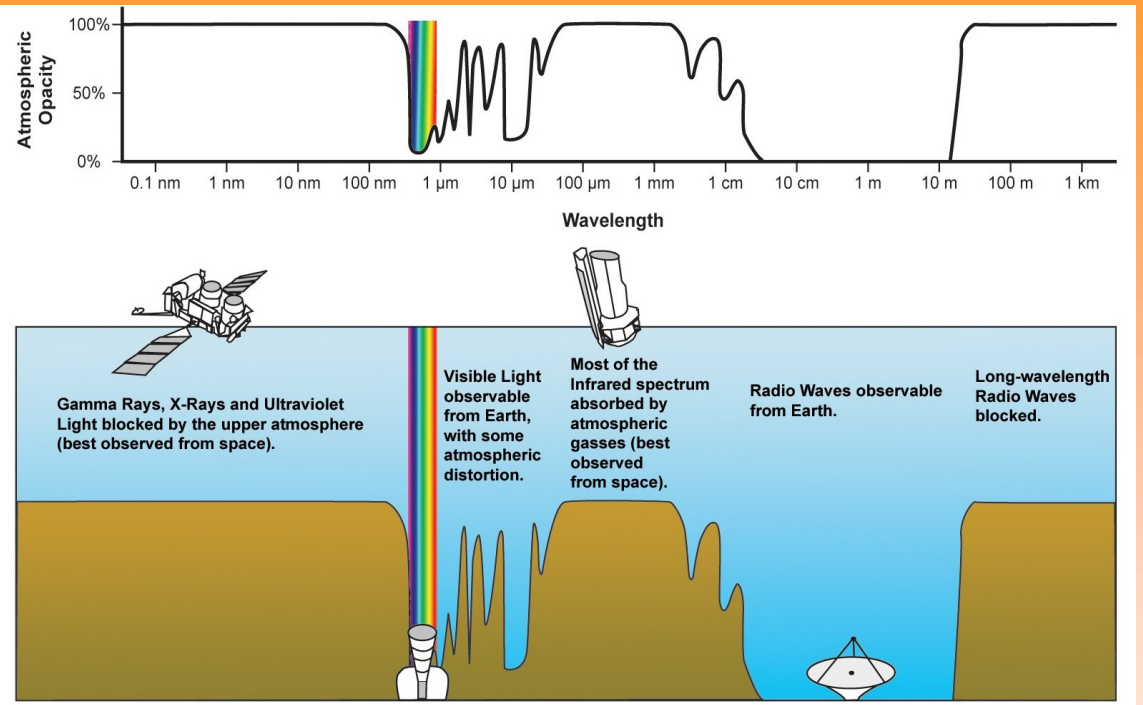

Main absorbers between the optical and radio transmission windows:

- H_2O ←
- CO_2

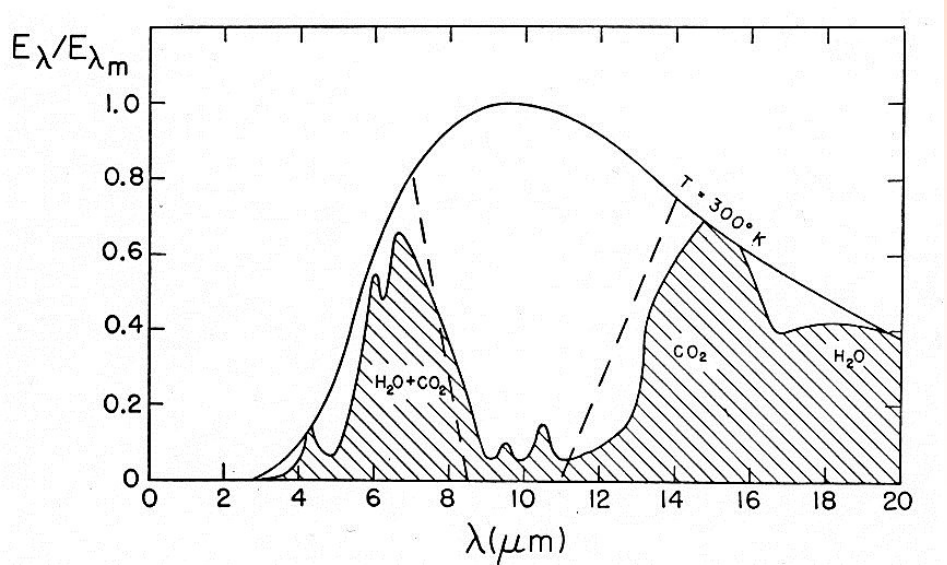

From:
Irbarne & Cho,
Atmospheric Physics

The physics behind the scenes

Water vapor produces radio seeing, but is invisible in the optical.
What happens between optical and radio wavelengths?

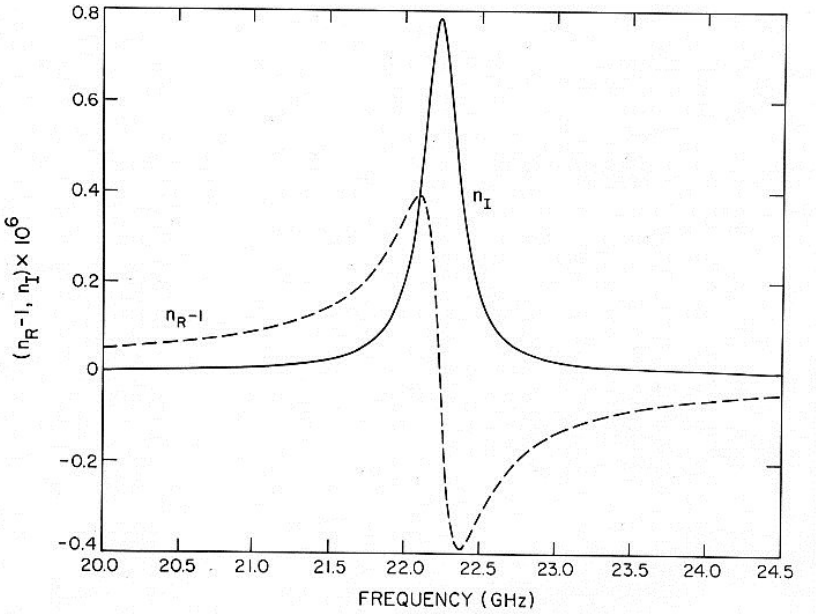

Figure 13.7 Real and imaginary parts of the index of refraction versus frequency for a single resonance given by Eqs. (13.63) and (13.64). The case shown is for the 6_{16}–5_{23} transition in *pure* water vapor with $\rho_V = 7.5$ g m^{-3}. In the atmosphere the line is much broader (Liebe 1969).

From: Thompson

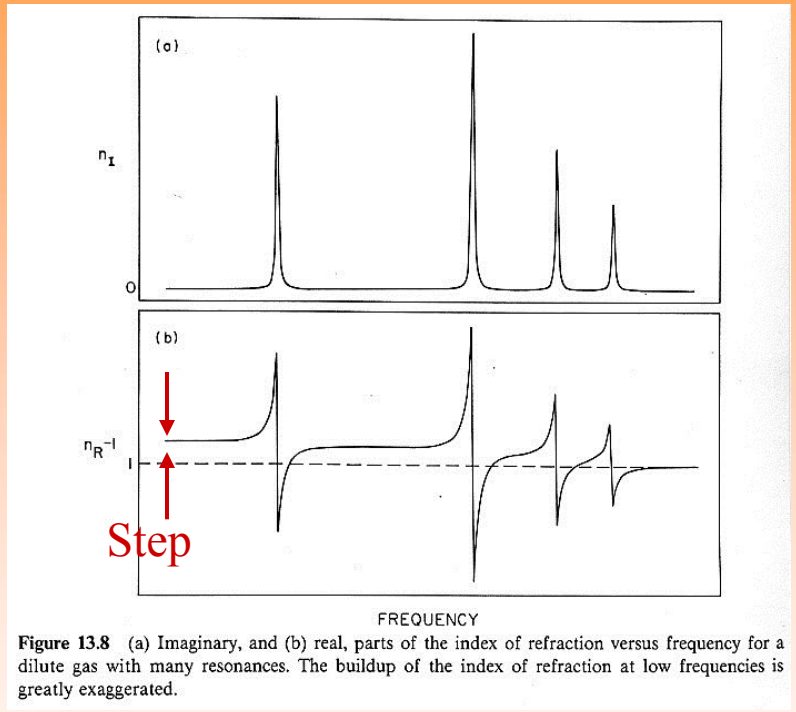

Figure 13.8 (a) Imaginary, and (b) real, parts of the index of refraction versus frequency for a dilute gas with many resonances. The buildup of the index of refraction at low frequencies is greatly exaggerated.

$$\chi_1(\omega) = \frac{1}{\pi}\mathcal{P}\int_{-\infty}^{\infty} \frac{\chi_2(\omega')}{\omega' - \omega}\, d\omega'$$

$$\chi_2(\omega) = -\frac{1}{\pi}\mathcal{P}\int_{-\infty}^{\infty} \frac{\chi_1(\omega')}{\omega' - \omega}\, d\omega',$$

The HITRAN2008 V13.0 database records 114,241,164 H_2O lines.

The extensive infrared H_2O absorption line system modifies the refractive index. (real and imaginary dielectric constants are connected over the Kramers-Kronig relations)

The physics behind the scenes

Troposphere: lowest atmospheric layer, about 10 km thick (varies with geographical latitude). Principal layer with humidity and weather patterns, and main source of mm amplitude and phase fluctuations. Temperature decreases by ~ -6.5°C / km with altitude ("lapse rate").

- Most of the solar radiation heats the ground, not the atmosphere it traverses
- Heat transport by convection, but most important mechanism by water vapor (evaporation, condensation, freezing).
- Day-to-day variations: planetary boundary layer, typically 1-2 km high, limited by a temperature inversion.
- Vertical temperature gradients are *less* than the adiabatic rate of 9.8°/km of dry air.

More details about water vapor:

- Molecular weight: 18.2 g/mol. In comparison, dry air has 28.96 g/mol
- Scale height H_0: 2 km. Dry air has 8.4 km *water: exp. profile on average only!*
- Mixes badly with dry air, has the tendency to separate and form bubbles of sizes between some cm and several km
- A "clear sky" in human terms can be full of turbulent water vapor, especially in summer.

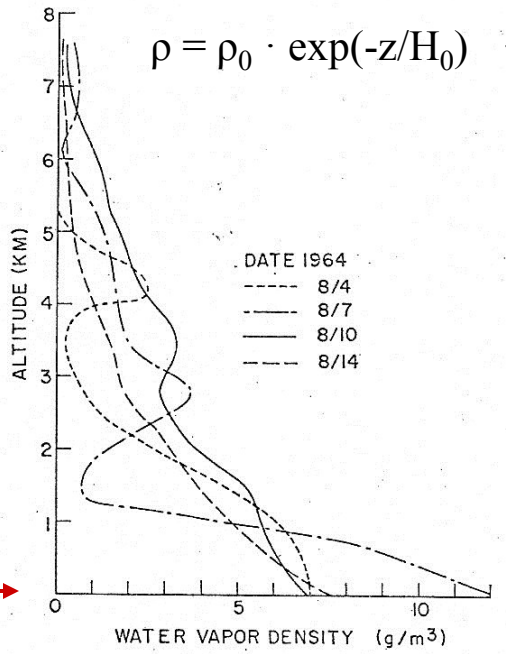

Fig. 3. Atmospheric water vapor profiles measured by radiosondes.

From: Staelin, 1966
(method: radiosondes)

The physics behind the scenes

Fig. II-3. *Average curves of temperature as a function of height at different seasons and latitudes.* On individual days, the temperature may vary considerably from these mean values.

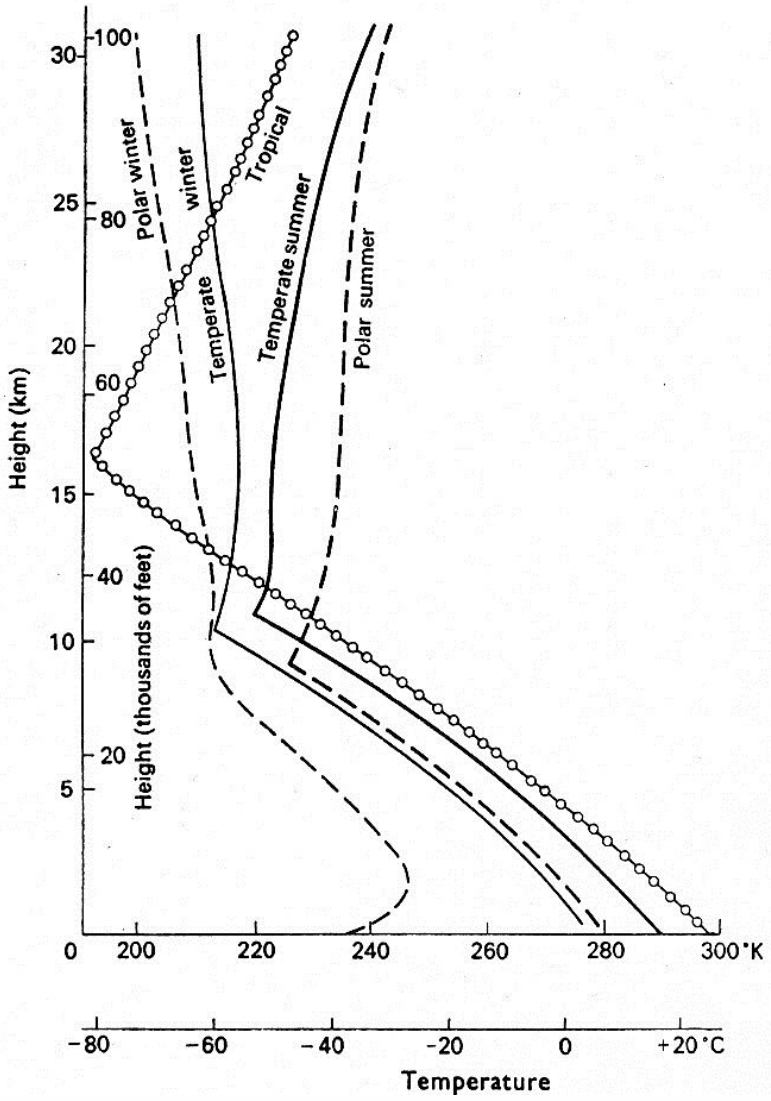

The vertical temperature inversion traps the water vapor, and keeps it from reaching altitudes where photo-dissociation can take place.

That happened apparently on Venus …

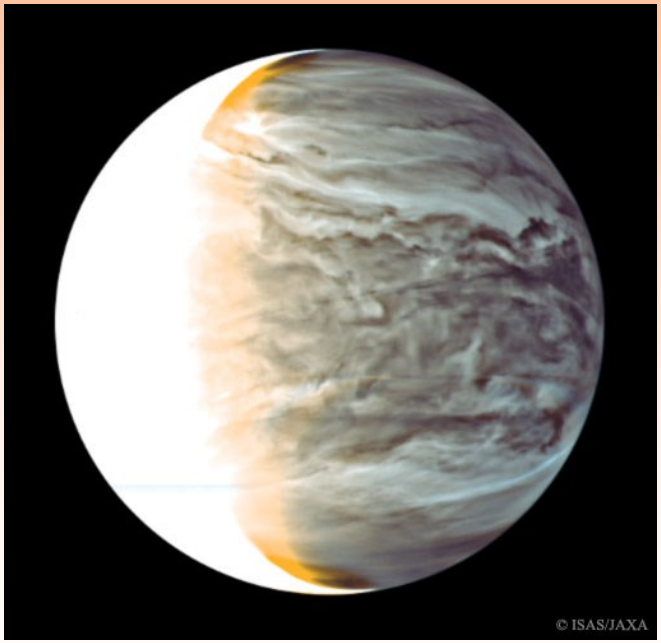

Venus in infrared, taken in April 2016 by the orbiting AKATSUKI spacecraft (ISAS/JAXA)

The physics behind the scenes

Can we predict numerically how the phase noise will be in some minutes? Is this easier or more difficult than a weather forecast?

For this line of argument, we are now entering …

Turbulent Times

A short look at the foundations of hydrodynamics:

Dynamics of viscous fluids have already intrigued Newton. The general equations for compressible viscous fluids (gases) are non-linear second order differential equations (Eq. 1.3).

$$\underbrace{\frac{d\vec{V}}{dt}}_{1.} + \underbrace{\frac{grad\, P}{\rho}}_{2.} + \underbrace{grad\, U}_{3.} \underbrace{- \frac{\eta}{\rho}\Delta\vec{V} - \frac{\xi + \frac{\eta}{3}}{\rho}\, grad\, div\, \vec{V}}_{4.} = 0 \qquad (1.3)$$

The various terms will be described in the following.

1. This part is the complete derivative in time, containing non-linear terms:

$$\frac{d\vec{V}}{dt} = \frac{\delta\vec{V}}{\delta t} + \left(\vec{V} grad\right)\vec{V} = \frac{\delta\vec{V}}{\delta t} + \underbrace{\frac{1}{2}\, grad\left(\vec{V}\cdot\vec{V}\right)}_{kin.\ Energy} \underbrace{- \vec{V}\times\left(curl\,\vec{V}\right)}_{Vortices} \qquad (1.4)$$

2. The pressure term describes the reaction to external forces, and is related to density and temperature over the equation of state.

3. External forces, described by the gradient of a Potential U. This form makes it easier to include this term into the others.

4. **Energy dissipation.** Viscous terms, with the Laplacian operator $\Delta = \nabla^2 = div\, grad$. The material constants η and ξ are the first and second viscosity coefficients, where ξ is specific to compressive media.

Turbulent Times

Is that really all … ?

To solve Equation 1.3, one needs:

- the equation of state for the gas,
- the conservation of mass and energy,
- the boundary conditions.

Considering the complexity of hydrodynamical phenomena, it was doubted for a long time if the equations could really be that simple.

Important: Many stationary solutions to problems are mathematically exact, but are not present in nature.

Turbulent Times

[Do simple equations always give simple answers?]

The now famous **Lorenz Attractor** was discovered by Edward N. Lorenz, who studied numerical solutions of a simplified meteorological convection problem.

$$\begin{aligned} x' &= -A \cdot x + A \cdot y \\ y' &= B \cdot x - y - x \cdot z \\ z' &= -C \cdot z + x \cdot y \end{aligned}$$

Lorenz obtained for $A = 10$, $B = 28$, $C = 8/3$ the following curve.

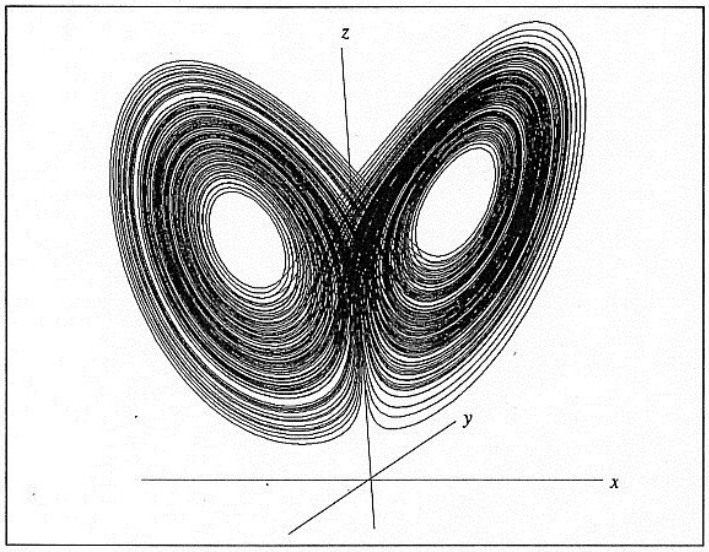

Lorenz E.N. (1963), Journal Atmos. Sci. **20**, 130

Simple nonlinear equations can produce very complex results.

The quadratic iterator $x_{n+1} = a \cdot x_n \cdot (1 - x_n)$**:**

- Very simple formula, easy to use.
  - Choose $a[0...4]$
  - start with a random $x_n[0...1]$
  - study x_n for $n > 100$
- Amazingly, lots of other non-linear formulas and very complex systems in nature mimic some of its properties.

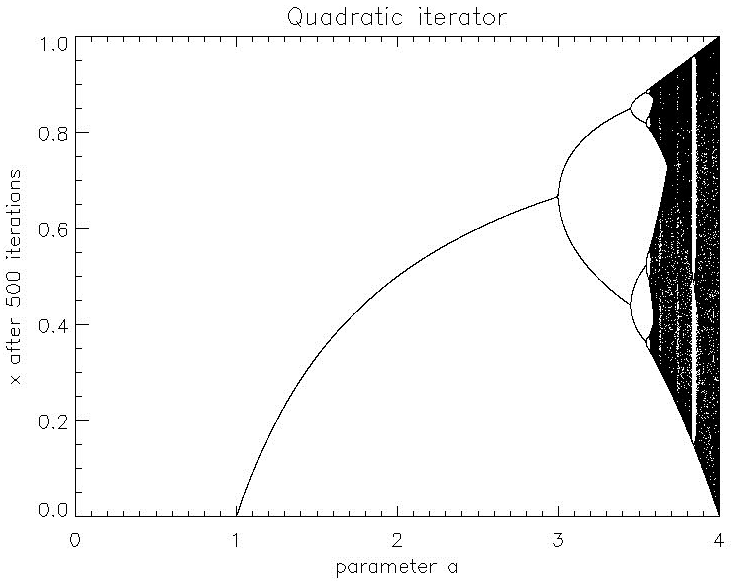

Turbulent Times

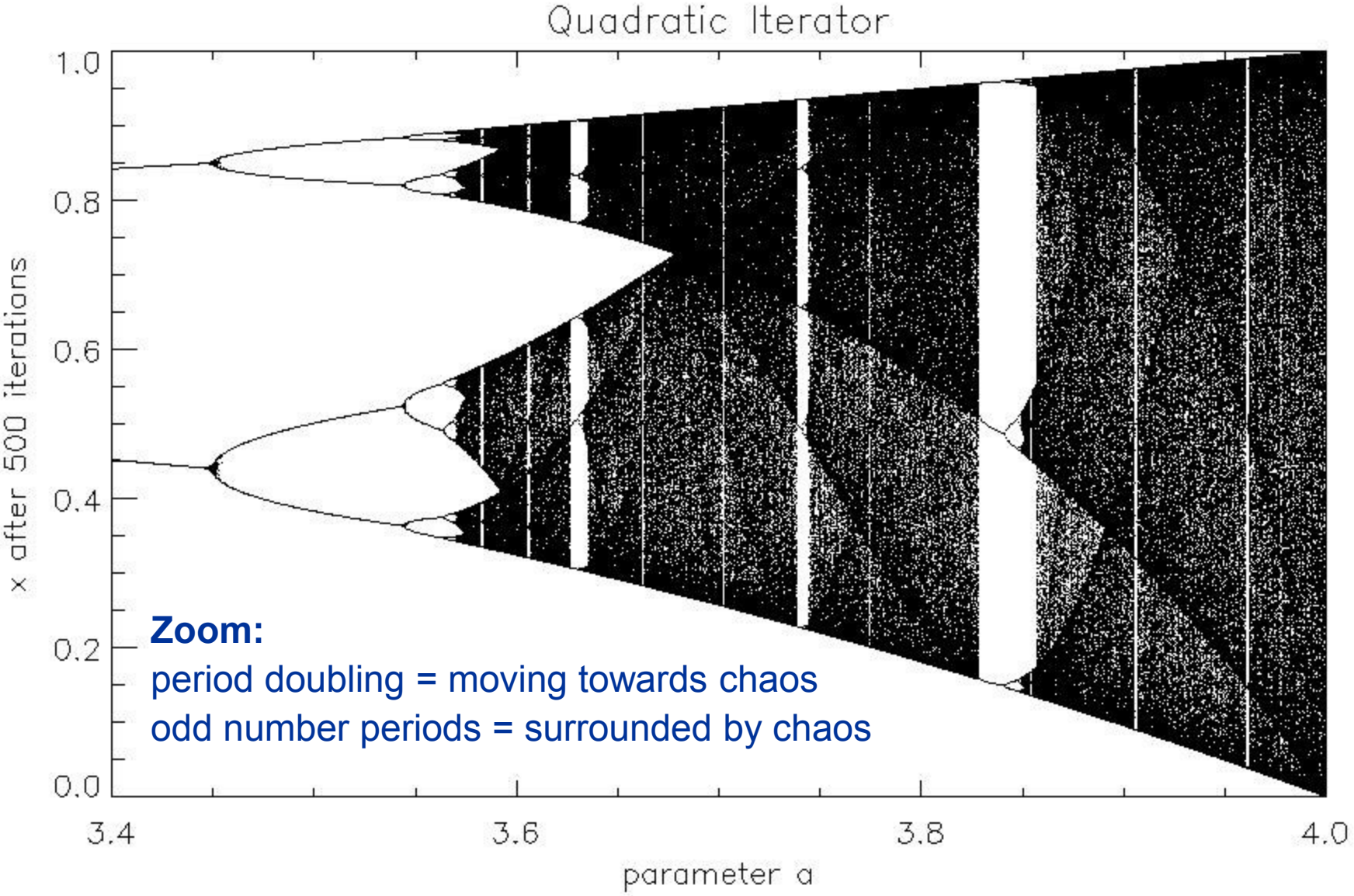

The Mandelbrot set – one of the most popular fractal structures.

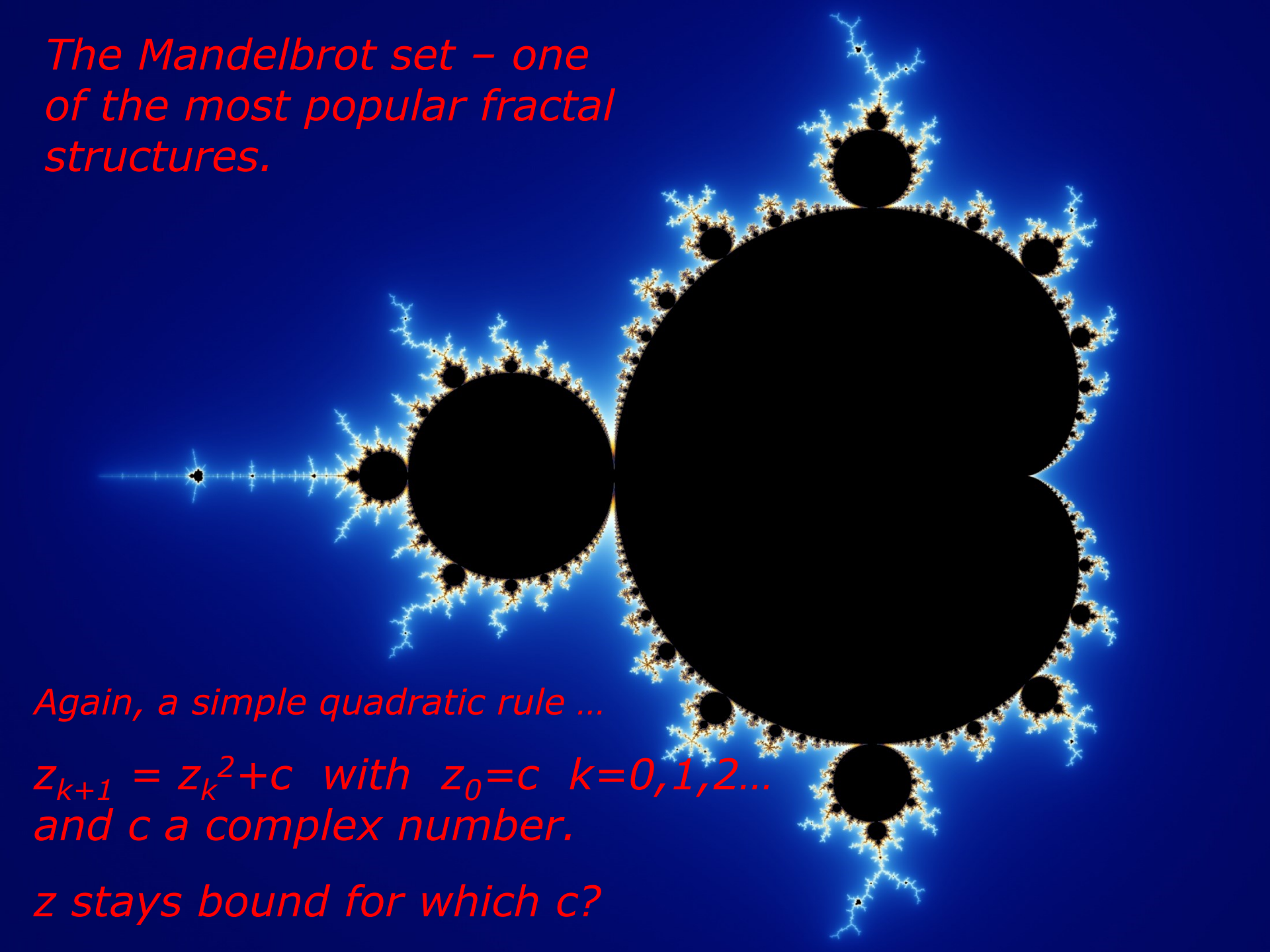

Again, a simple quadratic rule …

$z_{k+1} = z_k^2 + c$ *with* $z_0 = c$ $k = 0,1,2\ldots$
and c a complex number.

z stays bound for which c?

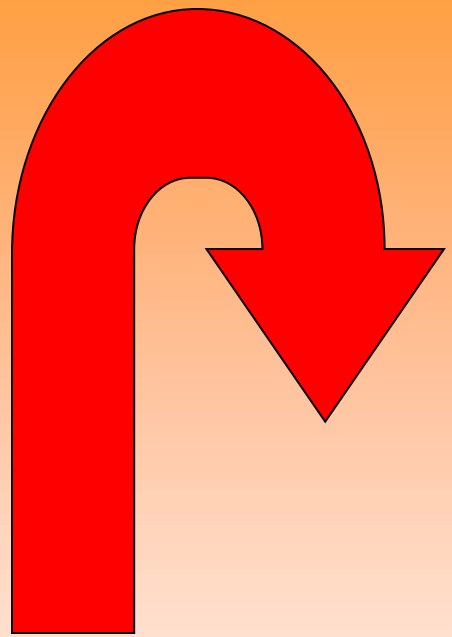

With some effort, we leave this tangent into fractals and get back to the hydrodynamics of turbulence.

Turbulent Times

Simplify Eq 1.3., and get the Law of Similarity:

1.3 Navier-Stokes equations, Reynold's Number

For most sub-sonic atmospheric flow problems, air can be treated as *incompressible medium*. The Navier-Stokes equations (Navier 1827, extended by Stokes in 1845) describe an incompressible medium with viscosity (Eq. 1.5).

$$\frac{d\vec{V}}{dt} + \frac{grad\, P}{\rho} + grad\, U - \frac{\eta}{\rho}\Delta\vec{V} \qquad (1.5)$$

Without external forces ($grad\, U = 0$), one can choose convenient units for spatial dimension and velocity:

- **Spatial dimension**: size of an obstacle in the flow l_0
- **Velocity**: flow velocity far from the obstacle V_0

i.e. one replaces the

- velocity V by $V' = V/V_0$
- spatial dimension l by $l' = l/l_0$,

which allows to change the other terms accordingly:

- time t by $t' = t \cdot v_0/l_0$
- density ρ by $\rho' = \rho \cdot l_0^3$
- pressure P by $P' = P \cdot l_0^3/v_0^2$

Turbulent Times

Finally one obtains the dimensionless equation

$$\frac{dV'}{dt'} + \frac{grad\ P'}{\rho'} - \frac{1}{Re}\Delta V' = 0$$

with the Reynold's number $Re = l_0 \cdot V_0 \cdot \rho/\eta$

If two systems have
the same geometry and Reynolds number,
their turbulent flows are alike,
no matter their relative size, viscosity or flow speed!

Critical Reynold's number Re_c: Problem dependent, typically between 10 and 100. For a given problem and a $Re > Re_c$, no stable solutions exist.

Medium	η [g/cm s]	$\nu = \eta/\rho$ [cm^2/s]
Water	0.010	0.010
Air	0.00018	0.150
Alcohol	0.018	0.022
Glycerin	8.5	6.8
Mercury	0.0156	0.0012

Table 1: Examples for viscosity and the kinetic viscosity $\nu = \eta/\rho$ from Landau-Lifschitz

Air and water: *obstacle of 5cm size in a flow of 5 cm/s speed: Reynolds numbers of 167 and 2500, respectively, i.e. turbulent flows rule in daily life.*

Turbulent Times

Example: Flow around a cylinder

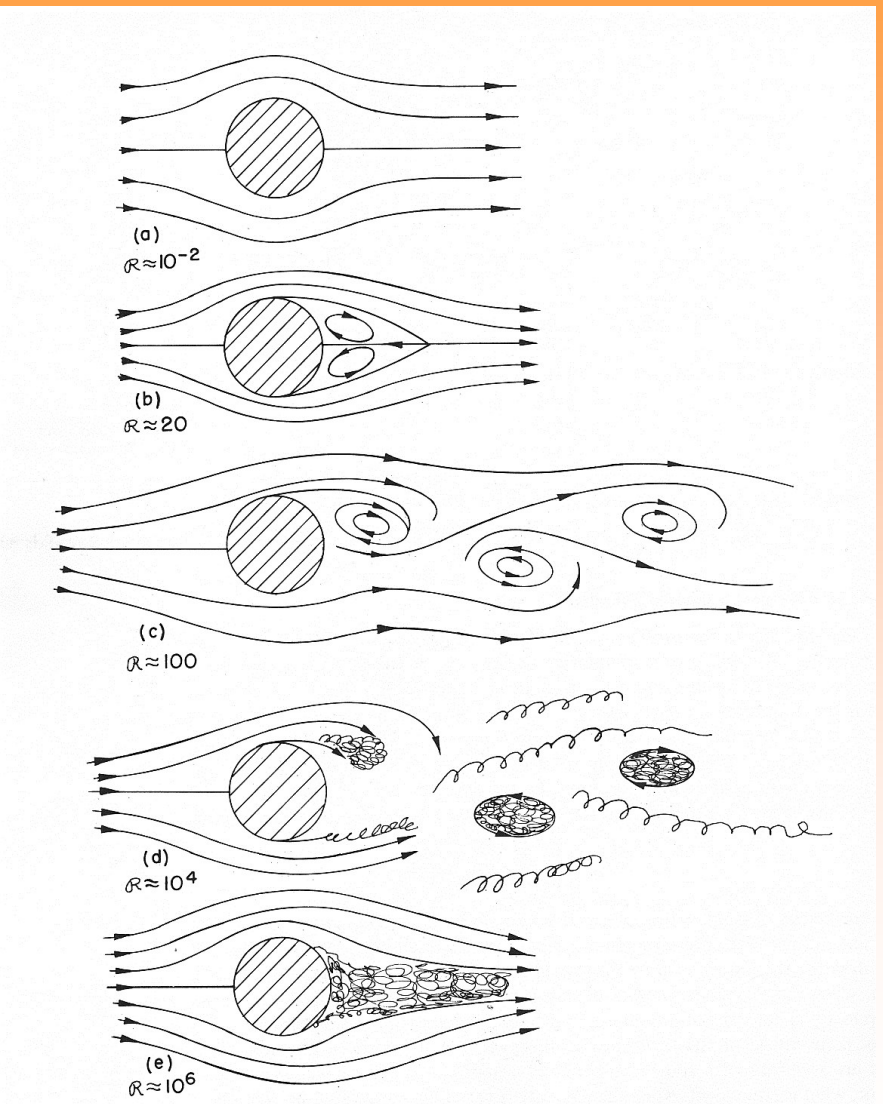

From: Feynman

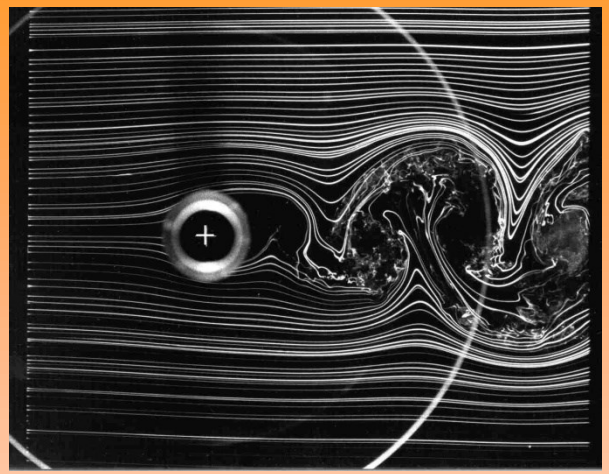

C.Norberg, LTH Lund, Sweden

NASA: Von Karman vortices off Rishiri Island, Japan

Turbulent Times

To come back to the question if we could predict phase noise numerically:

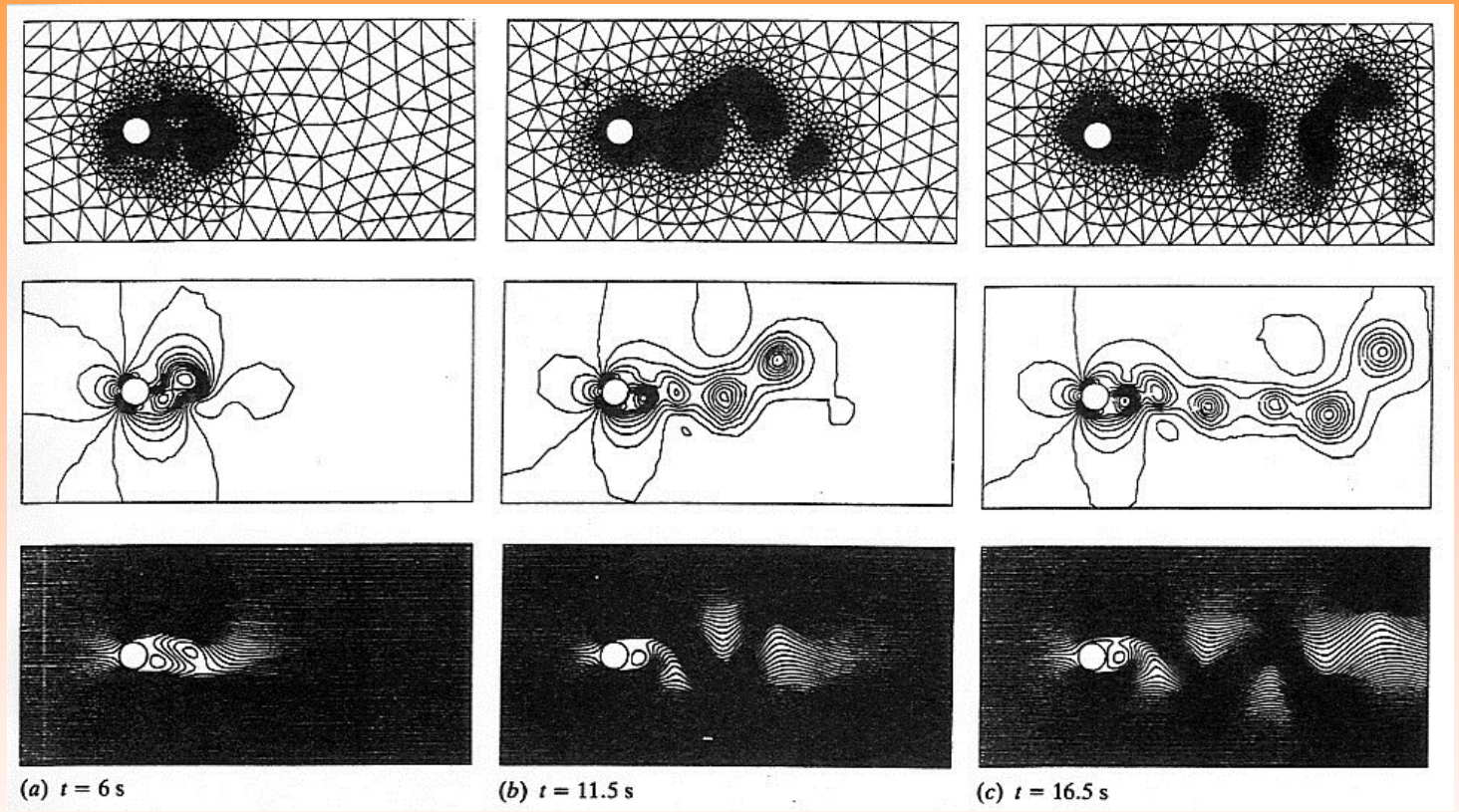

Already the turbulent flow around a cylinder with Re=250 is difficult to model and needs powerful adaptive grid methods. Imagine the leaves on a wind-moved tree …

Biggest problem: The boundary conditions (butterfly effect)!

Turbulent Times

What is the driving force behind turbulence?

Kinetic energy enters the flow system on a large scale, e.g. as convection or ground friction. Vortices form with high Reynolds numbers (*Re*).

The vortices fragment into smaller and smaller eddies with decreasing *Re* ("inertia range").

The smallest eddies have sub-critical Re, i.e. they dissipate their energy as heat ("viscous range").

Turbulence converts kinetic energy from large to small scale sizes, until it can be dissipated as heat.

Turbulent Times

We can examine the energy flow across the scales!

Kolmogorov (1941): For high R $(10^6 - 10^7)$, the turbulent structure of the inertia range is determined only by the **energy density for each scale size** ϵ and the **kinetic viscosity**. In the viscous range, it depends only on ϵ.

i.e., the smallest structures are homogeneous and isotropic.

Consequence for turbulence on intermediate scalesizes (when taking the simplest solution): Famous 2/3 law

$$D_{rr}(r) = C \cdot (\epsilon \cdot r)^{2/3} \tag{1.8}$$

Applies to fluctuations of temperature, velocity, ... Also for the refractive index.] thin layer, refractive index fluctuations and phase fluctuations are identical. This is the *thin screen approximation.*

$$D_{\varphi}(r) = C \cdot (\epsilon \cdot r)^{2/3} \tag{1.9}$$

For a thick turbulent layer, one obtains (after some calculations involving the spatial spectra and a Bessel function, see Tatarski (1961)) the form:

$$D_{\varphi}(r) = C \cdot (\epsilon \cdot r)^{5/3} \tag{1.10}$$

Turbulent Times

Statistical tools to analyze turbulence:

Structure functions: An instrument to characterize *non-stationary random processes*, first introduced by Kolmogorov (1941).

$$D_f(x_i, x_j) = \overline{(f(x_i) - f(x_j))^2}$$

Detailed theory based on random vector fields and their spatial spectra. Good reference, with theory and experiments:
Tatarski V.I (1961), Wave Propagation in a turbulent Medium, McGraw-Hill

Taylor's Hypothesis:
The turbulent structure changes on timescales that are long compared to the crossing time due to wind, and can be considered "frozen".

Relation between temporal and spatial structure function:

$$\overline{D}_\varphi(t) = \sqrt{(2)} \cdot D_\varphi(r) \mid_{r=v \cdot t}$$

The temporal structure function behaves well in the presence of noise.

Turbulent Times

Before we end this section, a small summary on what we have learned:

1. We cannot predict the future atmospheric phase noise from present values (no numerical “short term forecast approach”). The best we can do is direct measurement, and statistics.
2. Turbulence is a mechanism of energy dissipation. Wind, convection, cloud formation, mountains or big obstacles upwind etc. will increase phase noise. Nights and early mornings with little wind will typically have low phase noise.
3. To correct atmospheric phase noise, we need to monitor the atmosphere as close as possible to the optical path.

Monitoring

What Tool, please?

LIDAR (LIght Detection And Ranging)

Detection of atmospheric components over backscattering of laser light (directional, clear sky)

SODAR (SOnic Detection And Ranging)

Wind speed and turbulence detection over backscattering of sound (directional, limited range)

Radiometer (water vapor emission)

Thermal emission of water vapor and clouds (directional, quantitative)

Solar spectrometer (water vapor absorption)

Analysis of optical/IR absorption lines in front of a strong background source (quantitative, not directional, clear sky)

GPS (Global Positioning System)

Differences in GPS arrival times due to atmospheric path variations (quantitative, not directional)

Radiosonde (Balloons with sensor package)

In situ measurement of various atmospheric parameters (quantitative, not directional)

Monitoring: where to look

- Δ radio path ~ Δ quantity of water vapor along the line of sight
- water vapor emits in the radio range, we can measure Δ T(sky).
  - clear sky: Δ path ~ Δ vapor ~ Δ T(vapor) = Δ T(sky) *(easy)*
  - cloudy sky: Δ path ~ Δ vapor
    Δ T(sky) = Δ T(vapor) + Δ T(cloud) *(tricky)*

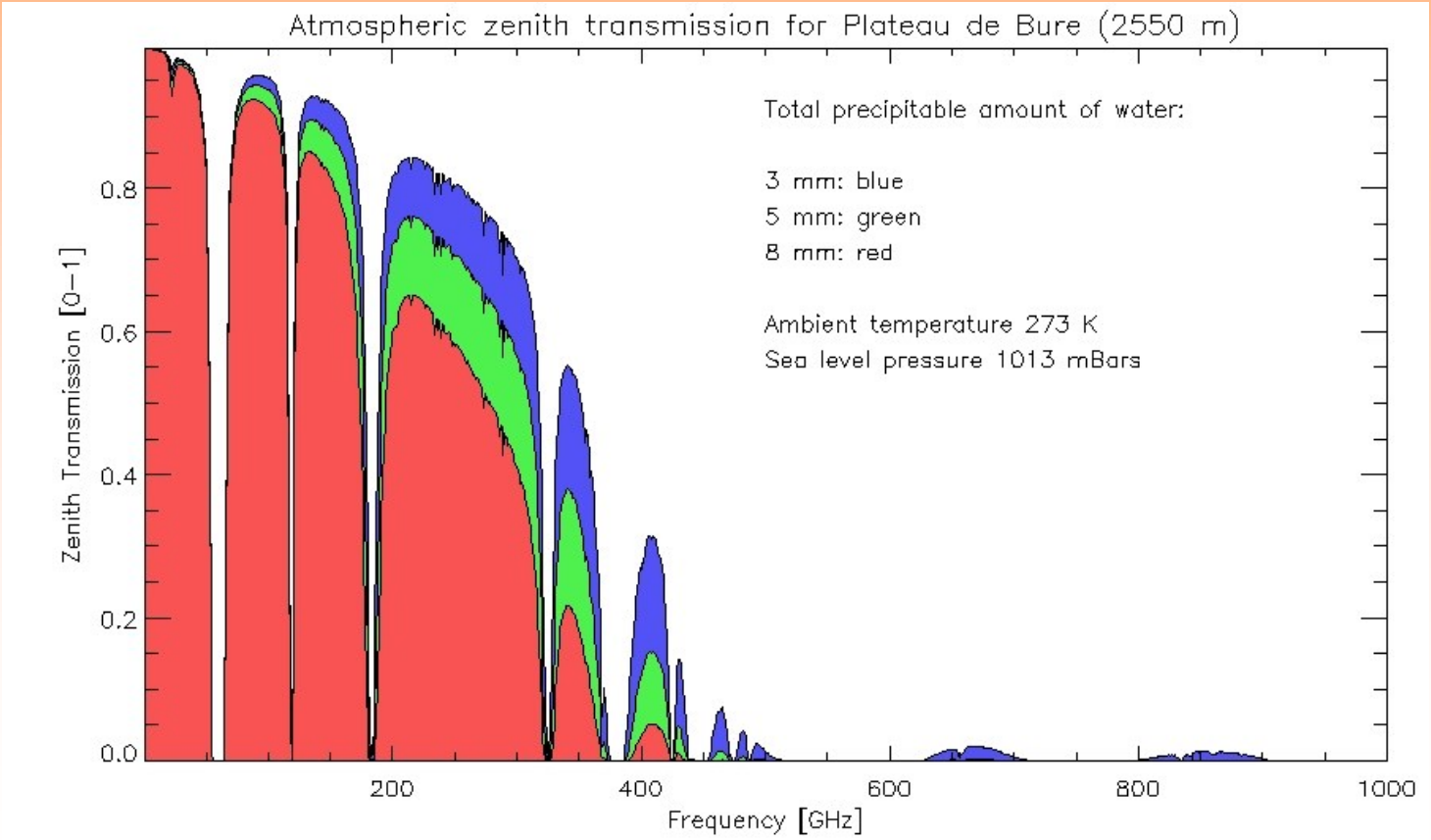

Monitoring: where to look

- Δ radio path ~ Δ quantity of water vapor along the line of sight
- water vapor emits in the radio range, we can measure Δ T(sky).
  - clear sky: Δ path ~ Δ vapor ~ Δ T(vapor) = Δ T(sky) *(easy)*
  - cloudy sky: Δ path ~ Δ vapor
    Δ T(sky) = Δ T(vapor) + Δ T(cloud) *(tricky)*

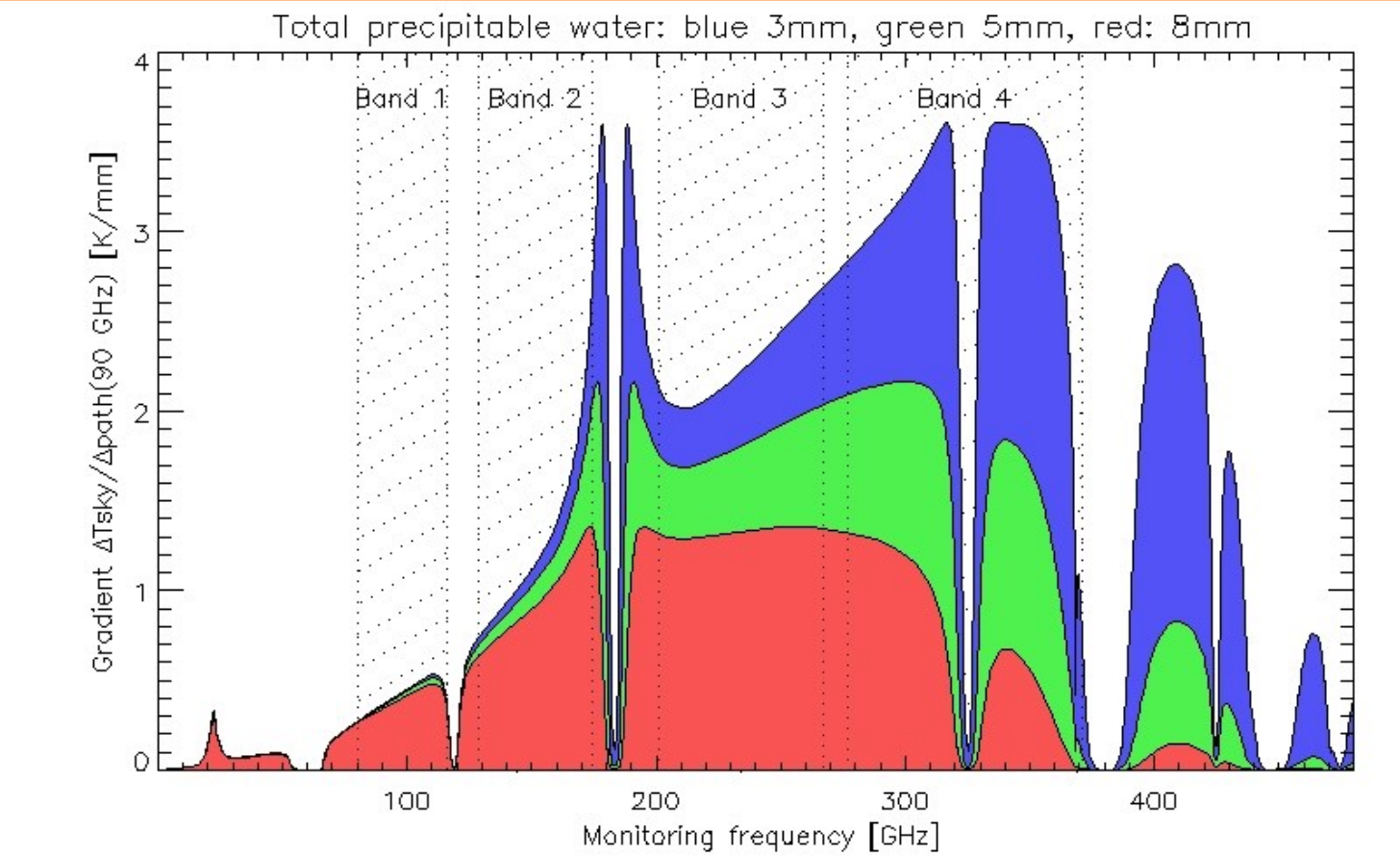

Monitoring: where to look

A word about Clouds:

- Clouds need humidity and condensation nuclei to form.
- Absorption coefficient is ~ υ^2 for observing wavelengths » drop size (Rayleigh scattering). Formalism for the general case: Mie scattering.
- Ice crystal clouds have little effect on phase noise
- A cloud layer indicates an atmospheric layer with droplets, saturated water vapour, and a higher temperature than a clear sky vertical profile would predict.

For monitoring purposes, it is easier to work in the Rayleigh scattering regime.

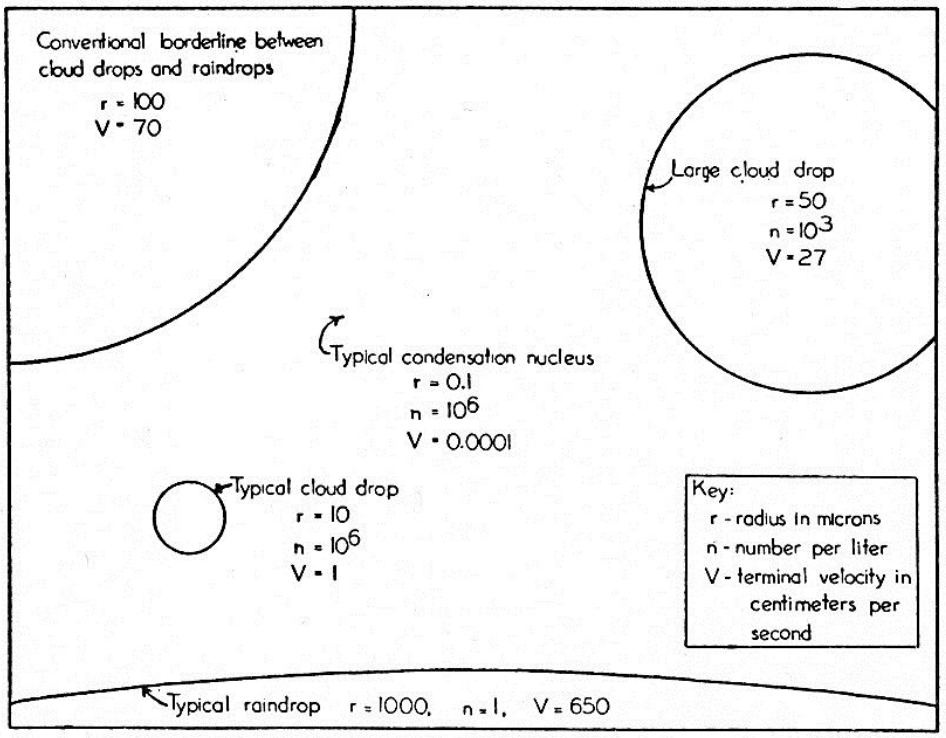

Fig. V-8. *Size range of elements involved in cloud physics.* Typical sizes, concentrations and falling velocities of nuclei, cloud droplets and raindrops.

Monitoring – practical implementation

Part 1: using the astronomical 1mm receiver signal

April 1995:	First PdBI phase correction (astronom. receiver at 230 GHz)
Nov. 1995:	Implementation into the real-time PdBI system
Oct. 1999:	Test of a 200 GHz VLBI phase correction at the IRAM 30-m
Oct. 2001:	Installation of the first 22 GHz radiometer on the PdBI
Dec. 2002:	Installation of the last 22 GHz radiometer on the PdBI
2003-2004:	Optimization of thermal and signal transport environment
June 2004:	Implementation into the PdB real-time system

Monitoring – practical implementation

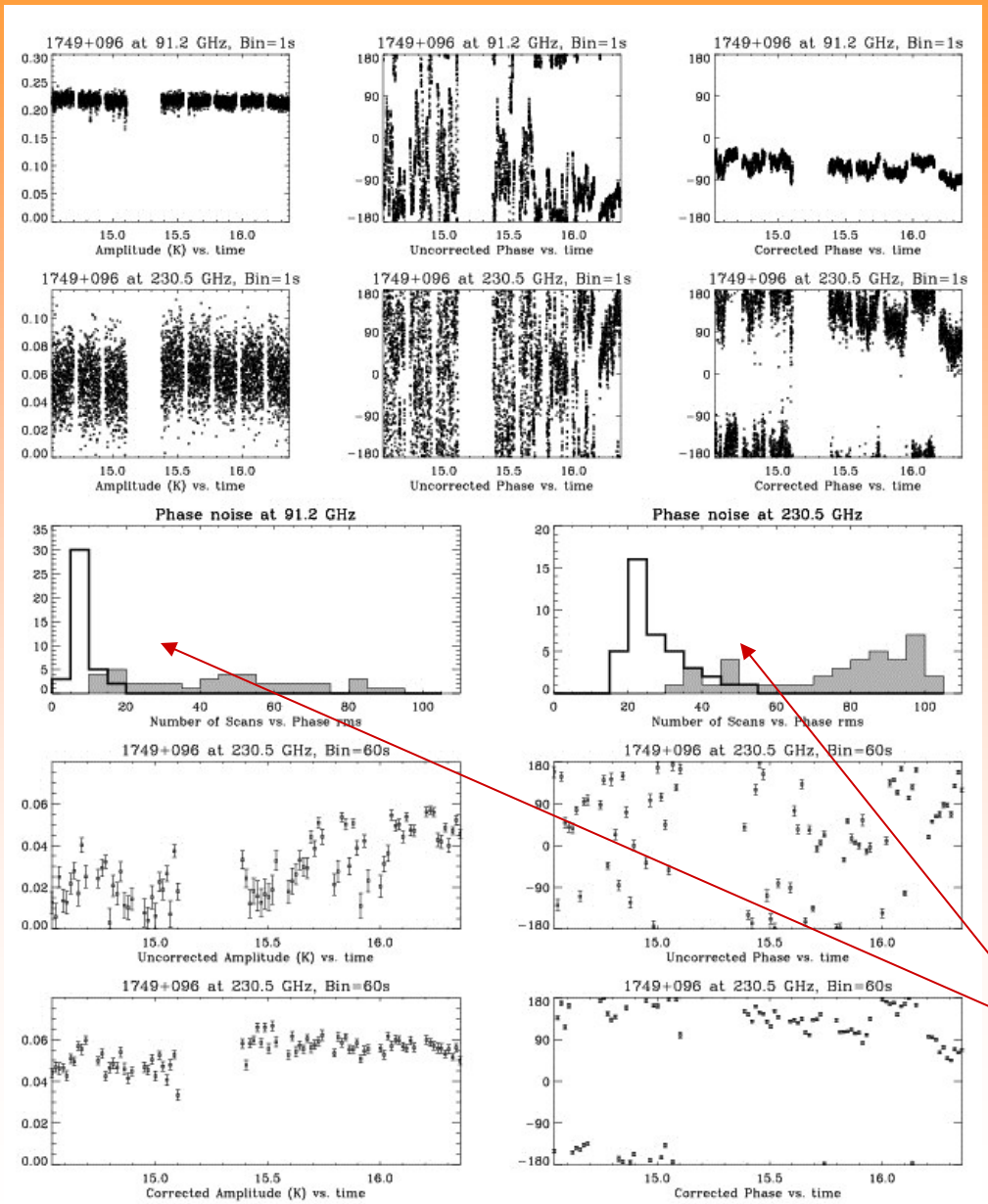

Astronomical receiver stability:

$2 \cdot 10^{-4}$ at 230 GHz

Differential Method:

determine the conversion factor c

$$\Delta path = c \cdot \Delta T_{sky}$$

from an atmospheric model,

store corrected and uncorrected data,

choose the data set with the highest amplitude in post-processing.

Discard corrected absolute phases.

Result:

Coherence is significantly improved under clear sky conditions.

grey = uncorrected,

white= corrected phases

Monitoring – practical implementation

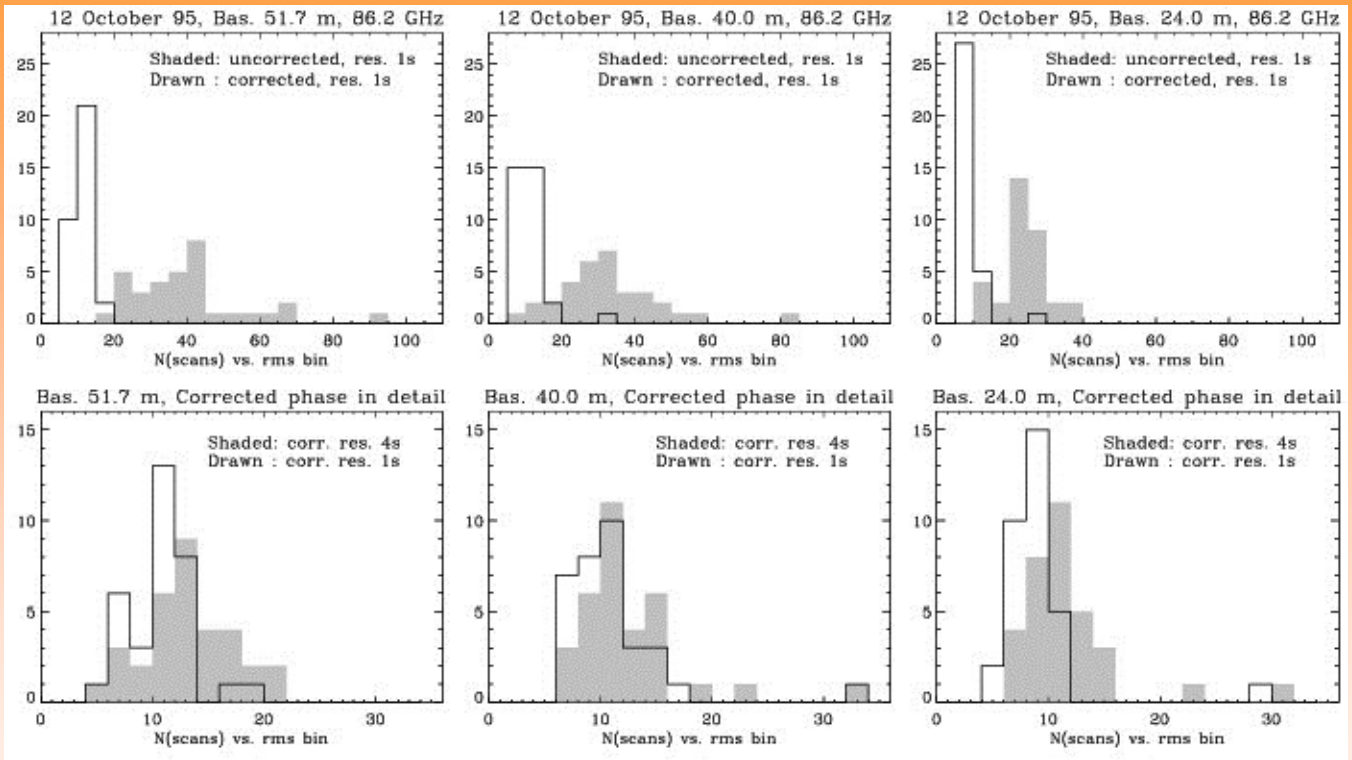

Comparison of the phase correction at 1 second and 4 seconds time resolution:

4 seconds: better S/N of the averaged total power signal.

1 second: better time resolution.

The higher time resolution gives better results.

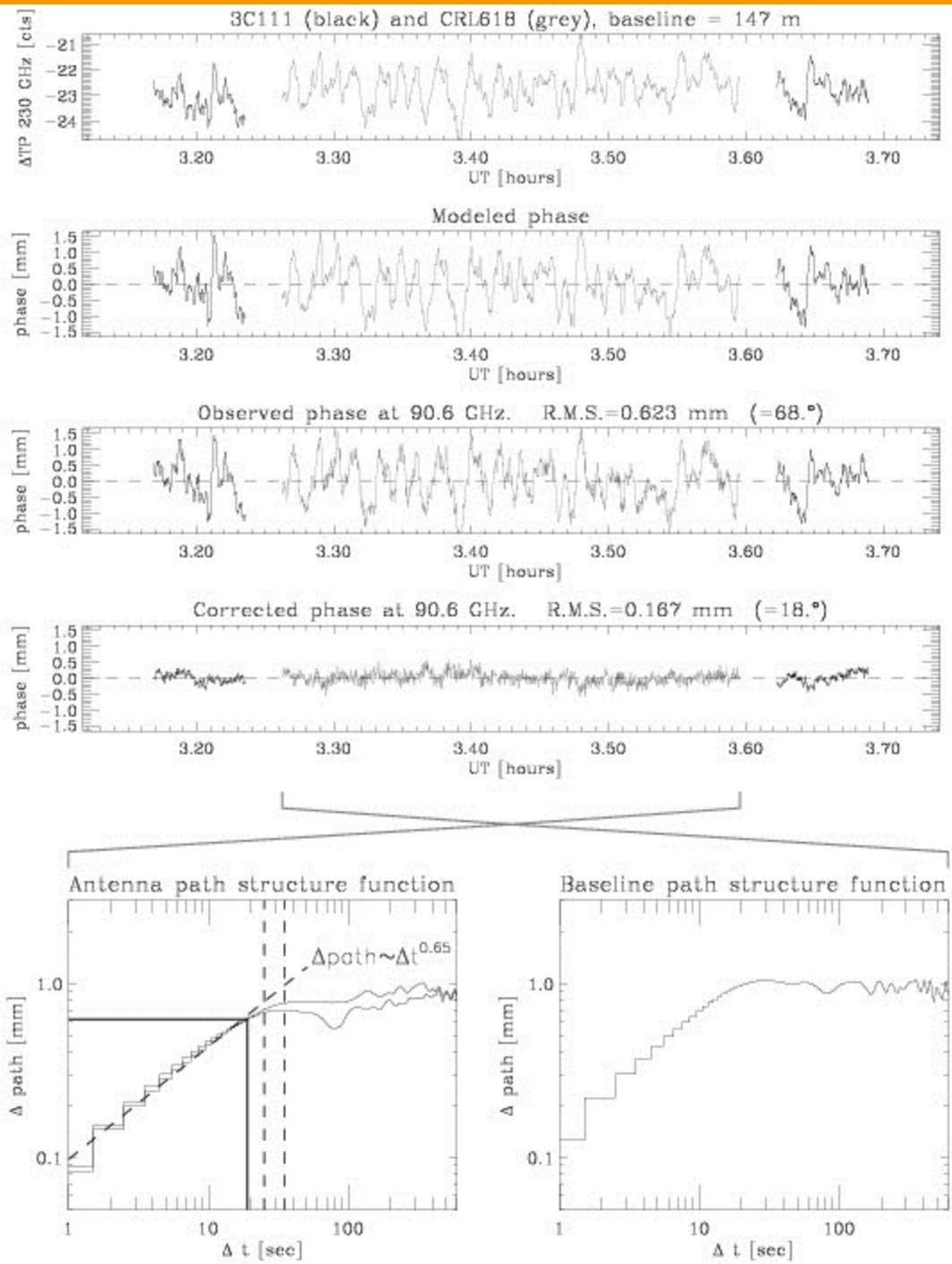

Example

Clear sky phase modeling was successful with the ATM atmospheric model by Chernicharo (1985).

Note:

We are using at present an updated version of ATM by Juan Pardo.

Monitoring – practical implementation

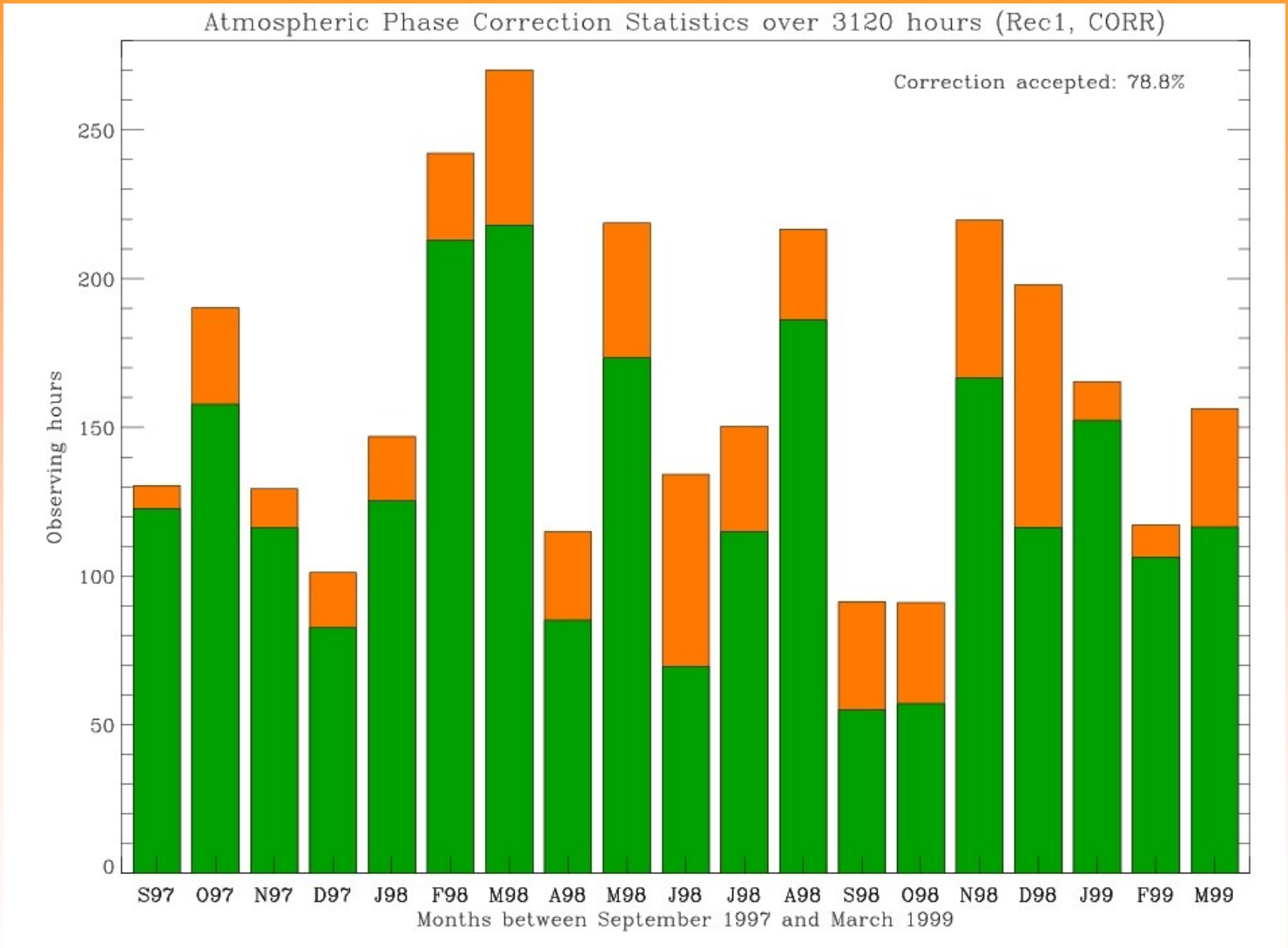

Result: Differential phase correction is successful most of the time.

If it works so nicely,
why change to a 22 GHz system?

Drawbacks of the 1mm phase monitoring:

1. Additional tuning time to optimize the astronomical 1mm receivers for total power stability
2. Concerns that the following receiver generation with closed-cycle Helium cryostats may be more instable in total power
3. Gain-elevation variations show hysteresis effects, no continuous phase tracking over source changes possible (this would be absolute phase correction)

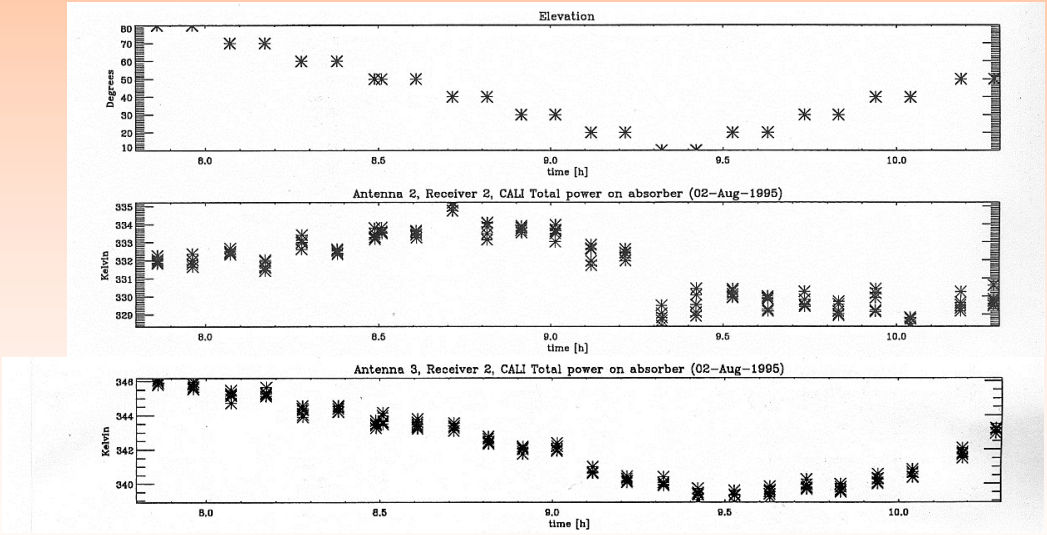

4. Clear sky phase correction only

Clear sky, cloudy sky

Monitoring in the 1mm continuum band:

No straight-forward detection of clouds.

Consequences:

No clouds (monitoring improves data)

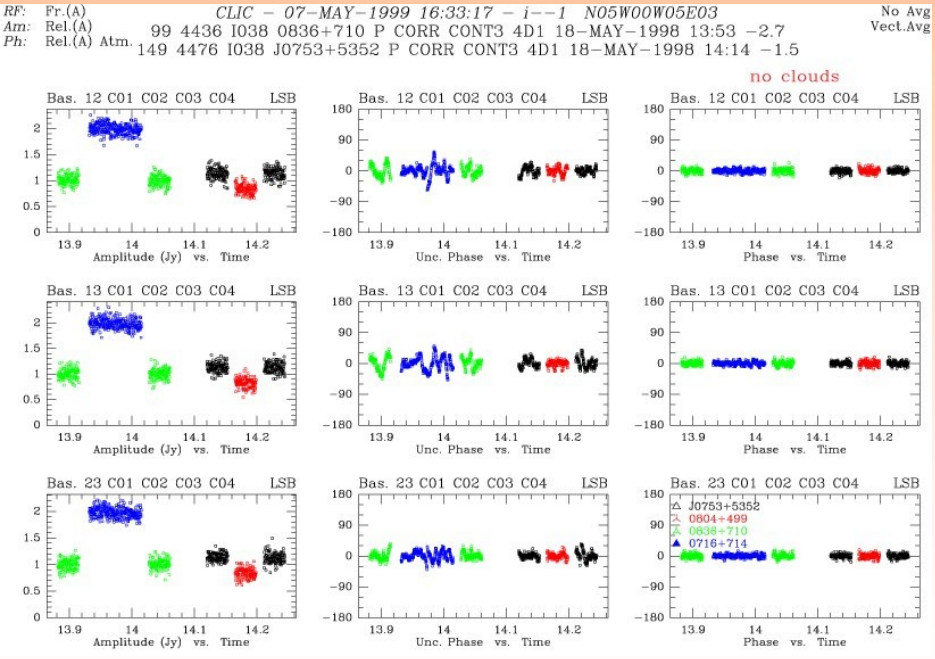

Clouds (monitoring degrades data)

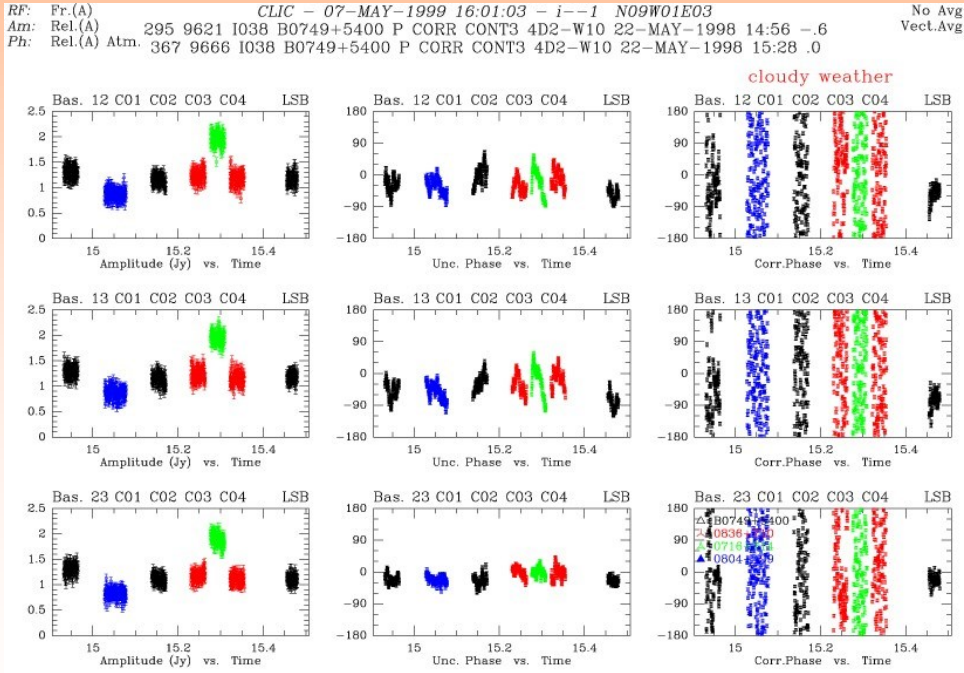

Monitoring – practical implementation

April 1995: First PdBI phase correction (astronom. receiver at 230 GHz)
Nov. 1995: Implementation into the real-time PdBI system
Oct. 1999: Test of a 200 GHz VLBI phase correction at the IRAM 30-m

Part 2: Using a dedicated 22 GHz system

Oct. 2001: Installation of the first 22 GHz radiometer on the PdBI
Dec. 2002: Installation of the last 22 GHz radiometer on the PdBI
2003-2004: Optimization of thermal and signal transport environment
June 2004: Implementation into the PdB real-time system

A dedicated 22 GHz WVR

Requirements for phase correction:

- Observing and monitoring beams must be close together

  Beware of effective baselines at the altitude where observing + monitoring beams cross the phase screen:

  15 arcmin separation = 17 meters at 4 km distance would be nice

  5 degrees separation = 340 meters at 4 km distance would be useless

- Data rate of 1 readout /second
- Receiver parameters (gain, T_{rec}) should not depend on elevation.
  If this cannot be avoided, they must have no hysteresis to allow calibration.
- Receivers of high intrinsic stability required.

This is the "wish list" which goes to the receiver group …

Bure 22 GHz radiometers: parameters (I)

- Ambient temperature, Peltier-stabilized instrument
- Absolute stability (30 min): $7.5 \cdot 10^{-4}$, differential stability (between channels): $8 \cdot 10^{-5}$
- Measured receiver temperatures of the 6 radiometers: 170 K - 220 K
- Separation between observed and monitored optical axis: 15' Azimuth,
  The WVRs use the astronomical Cassegrain main reflector / subreflector
- Monitoring data recorded once per second

And this is what comes back!

Bure 22 GHz radiometer: parameters (II)

- Cloud opacity is ~ υ^2 for wavelength » droplet size.
- All exponential terms at 22 GHz can be linearized for realistic observing conditions at 82 GHz.
- $T_{wvr} = F_{eff} \cdot (T_{vap}+T_{cloud}) +(1-F_{eff}) \cdot T_{amb} + T_{rec}$

Then the combination of 3 channels

$$T_{triple} = (T_1 - T_2 \cdot \upsilon_1^2/\upsilon_2^2) - (T_2 - T_3 \cdot \upsilon_2^2/\upsilon_3^2)$$

removes cloud emission and constant temperature offsets if

$$\upsilon_1^2/\upsilon_2^2 = \upsilon_2^2/\upsilon_3^2$$

22 GHz radiometer: parameters (III)

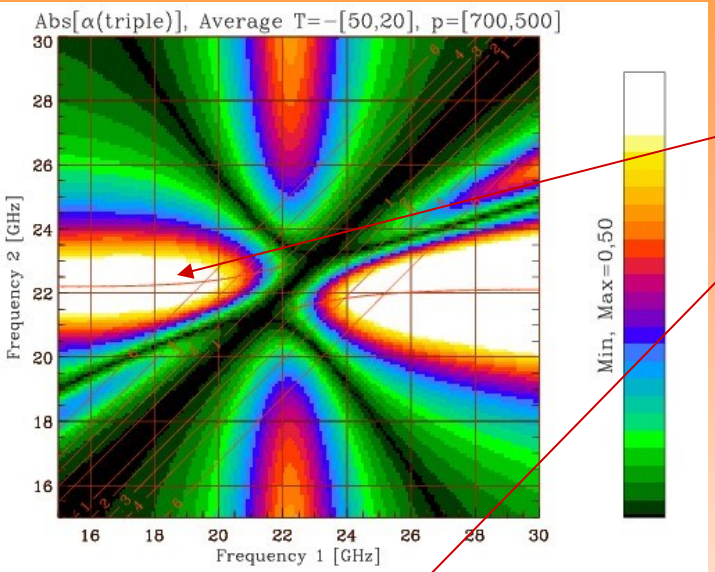

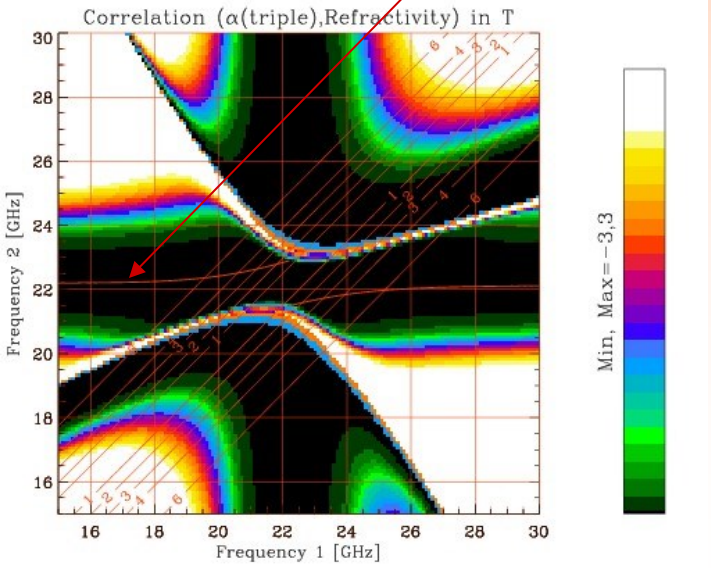

In the graphs, $\upsilon_3 = \upsilon_2^2/\upsilon_1$

Traced ridges: maximum sensitivity

Conflict with a minimum dependency of the optical path on vertical atmospheric temperature.

Maximum sensitivity was preferred.

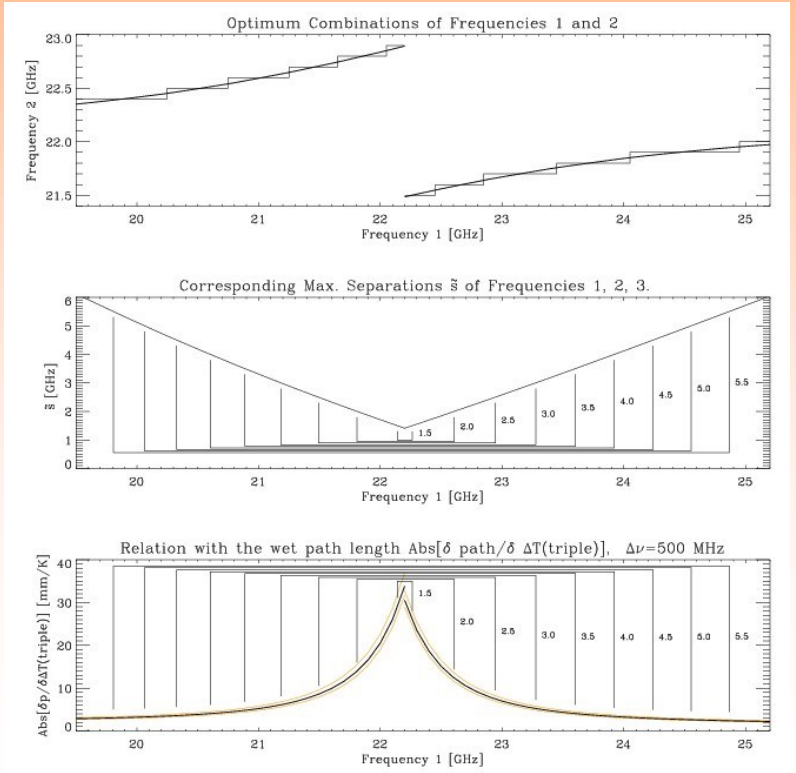

22 GHz radiometer: parameters (IV)

Choice of frequencies for the Plateau de Bure Radiometers:

Three channels of 1 GHz bandwidth each:

υ_1=19.175 GHz , υ_2=21.971 GHz , υ_3 = 25.175 GHz

Selected by fixed filters on the 8 GHz bandpass of a single receiver.

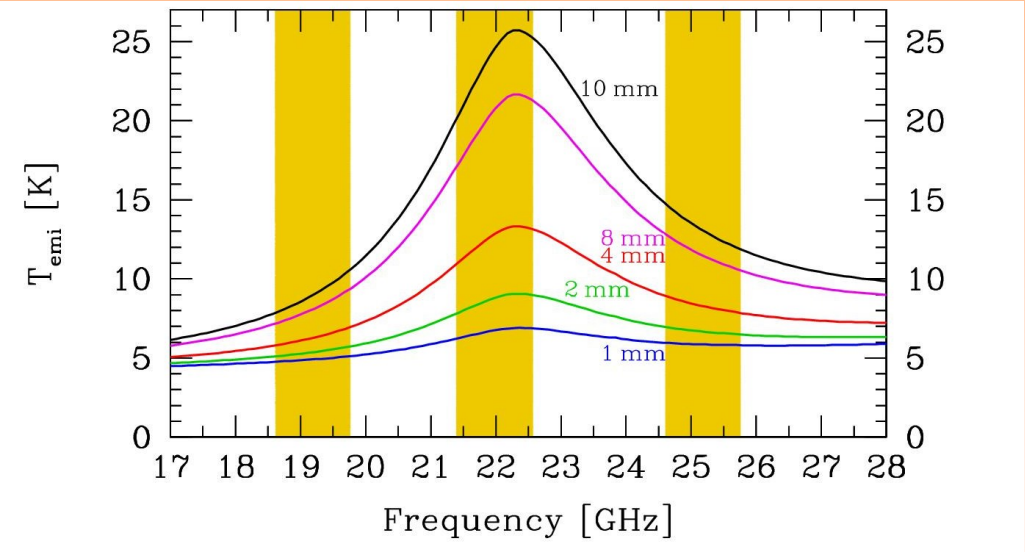

It was not possible to stay on ITU protected frequency bands to reach the required sensitivity.

Calibration hardware: a waveguide-mounted noise diode and an ambient load table.

22 GHz radiometer – some photos

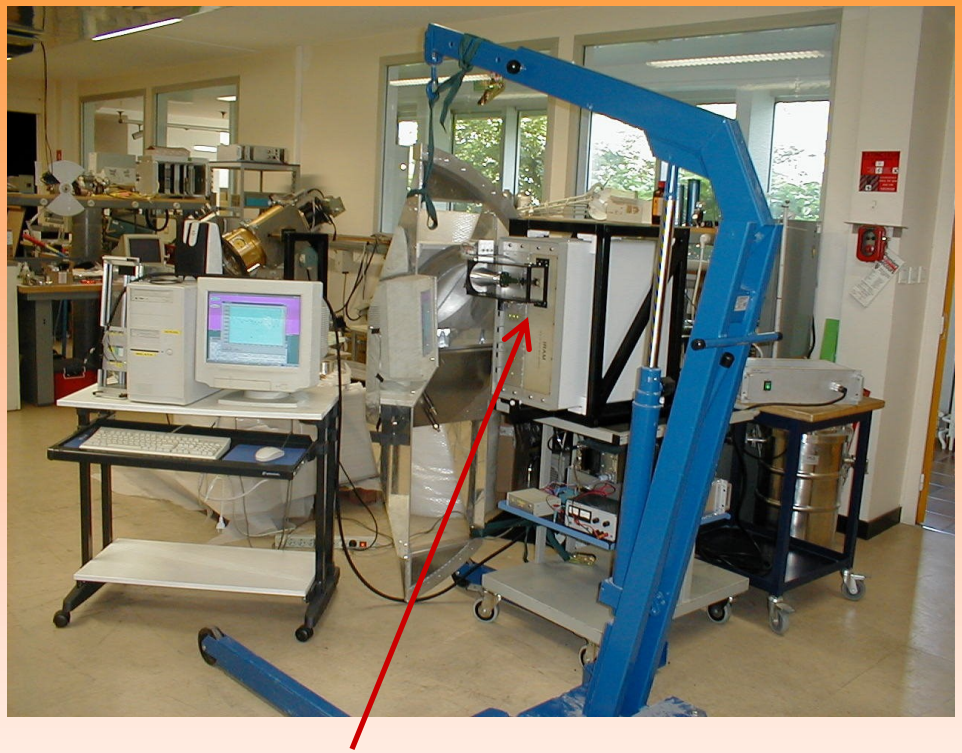

22 GHz Radiometer in the Grenoble receiver labs. Part of a receiver cabin wall (vertex-side) is suspended from a crane to study the mirror system which approaches the monitoring and observing beams.

Three radiometers in a row in the Grenoble receiver labs. Tests before crating and transport to the Plateau de Bure.

22 GHz radiometer – practical implementation

Here an example of the application of the phase correction:

significant improvement!

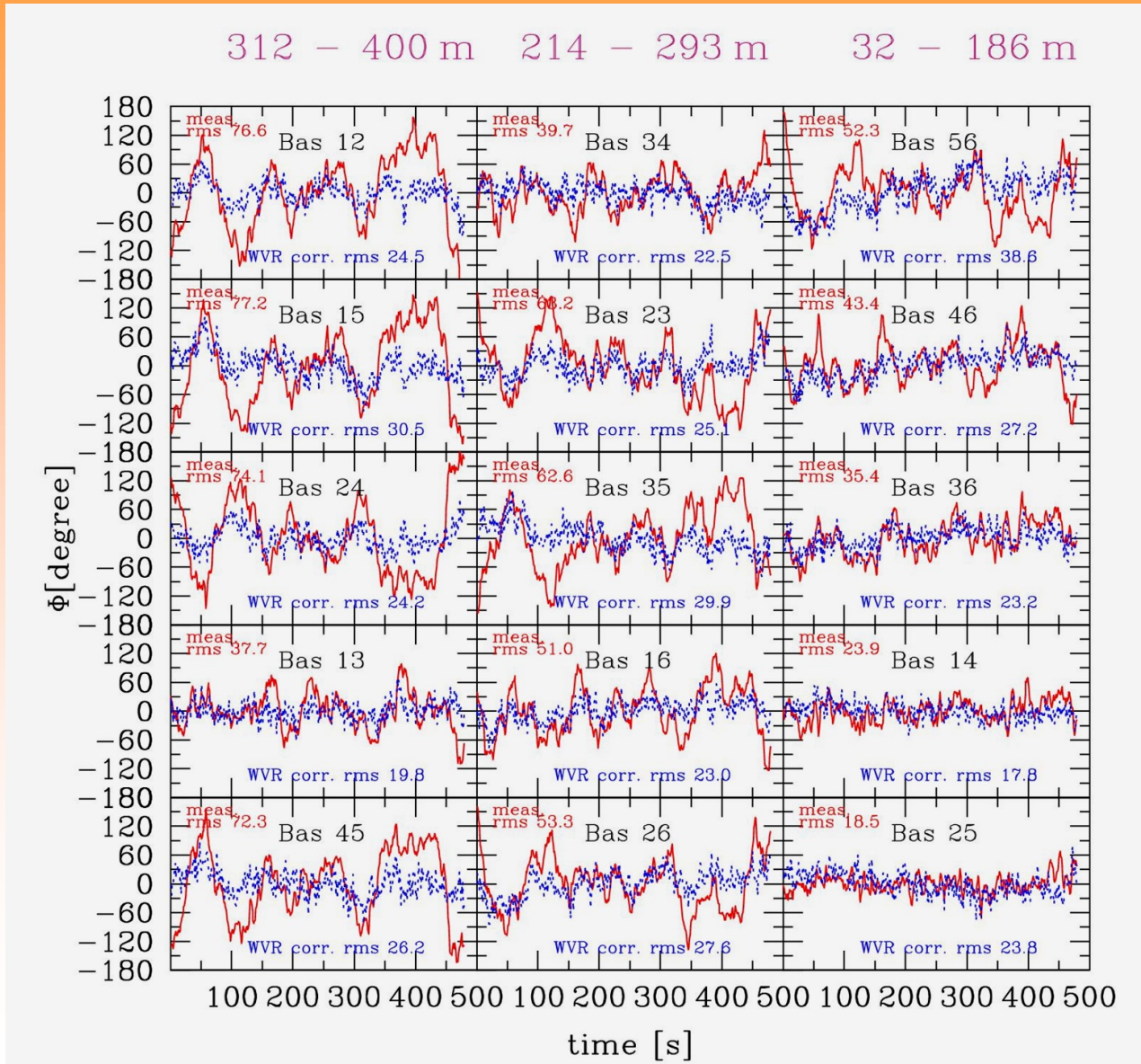

22 GHz radiometer – practical implementation

Our example on MWC349 from the beginning:

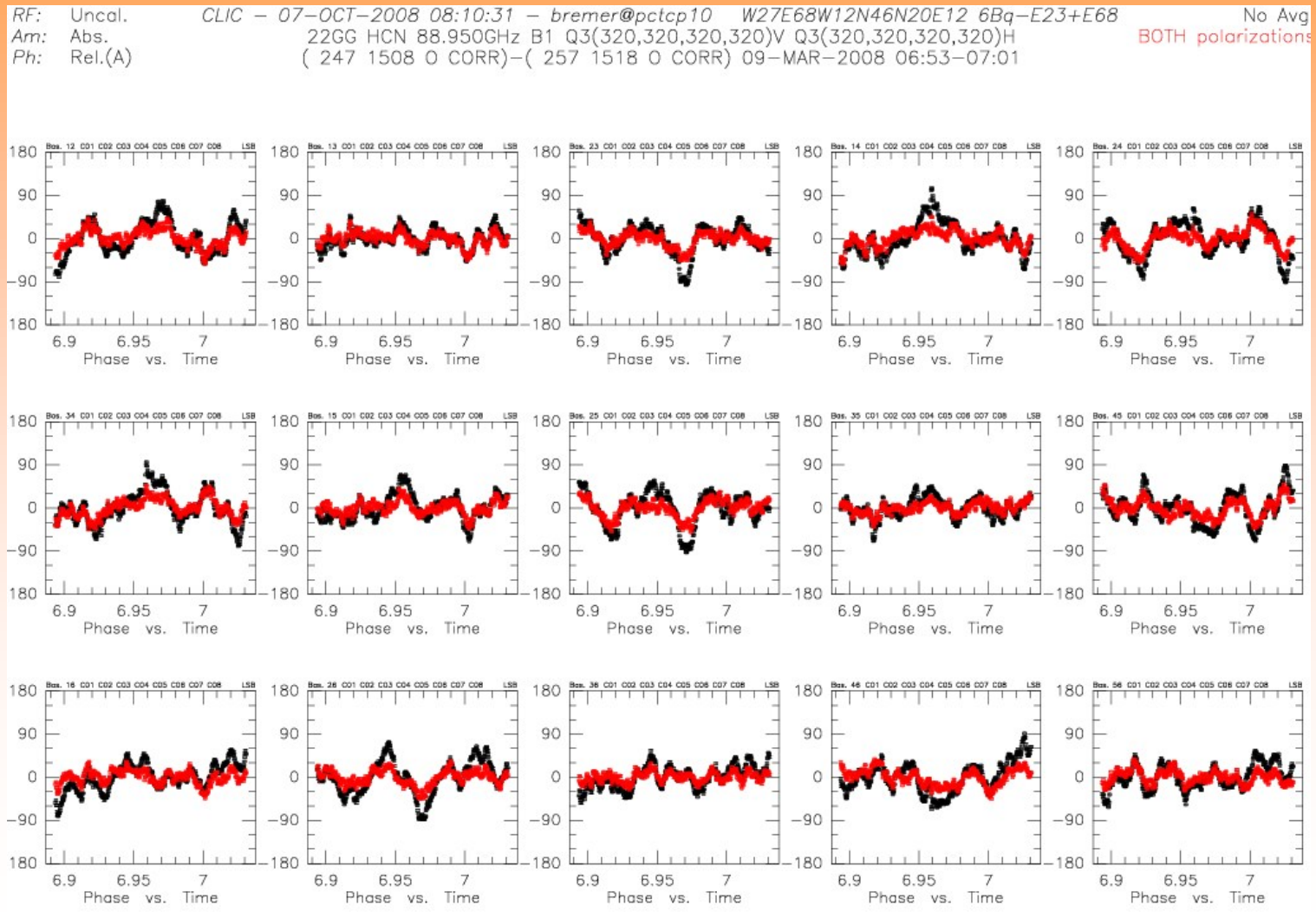

22 GHz radiometer – practical implementation

The corresponding phase noise vs. projected baseline plot:

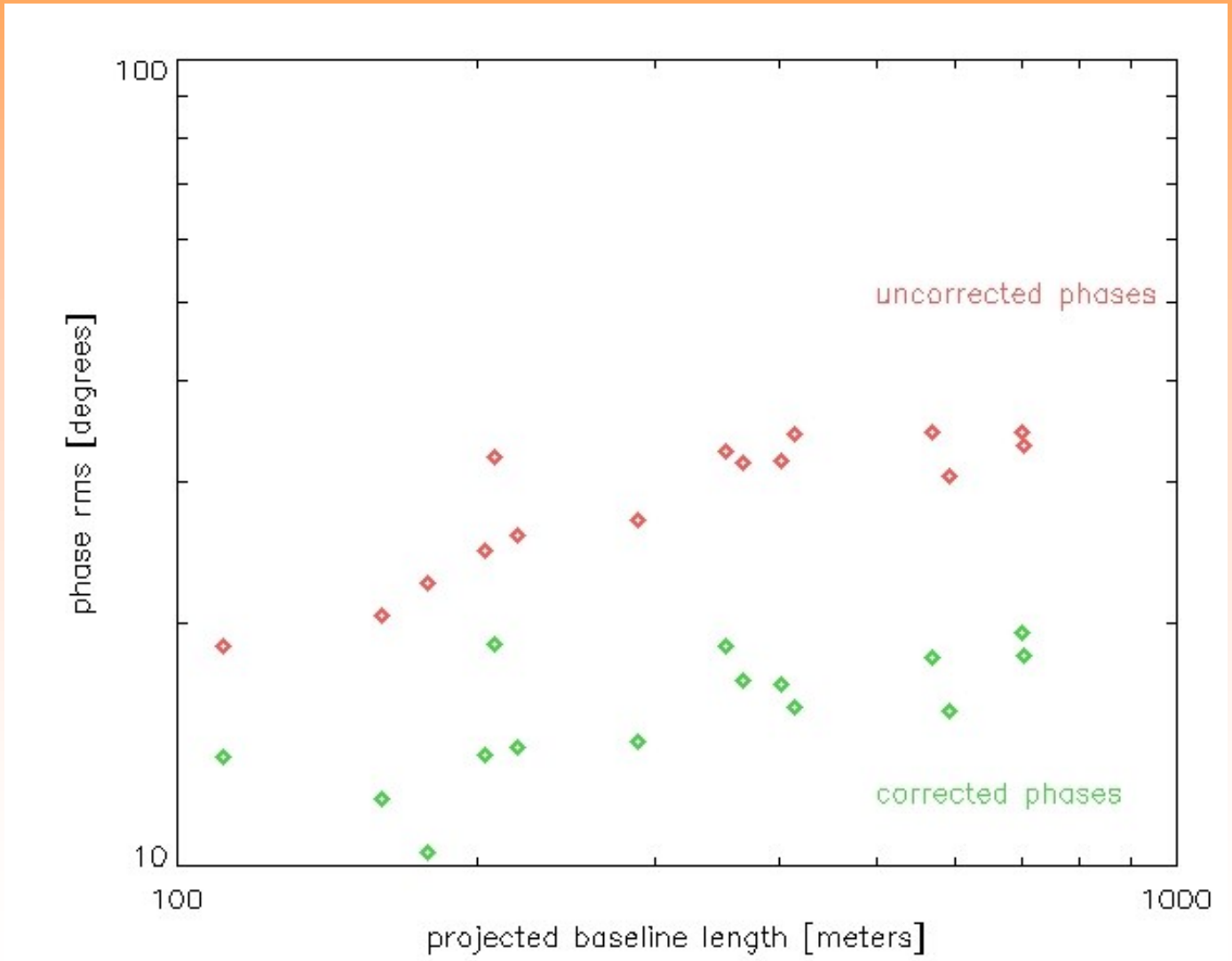

22 GHz radiometer – practical implementation

Standard of the PdBI “default” phase correction:

We still discard the corrected phases and only keep the improved amplitudes.

Why?

All residual error terms of the radiometers would appear in the phases. We are developing automated checks.

Once these options are safe, we will release them.

WVR phase correction statistics

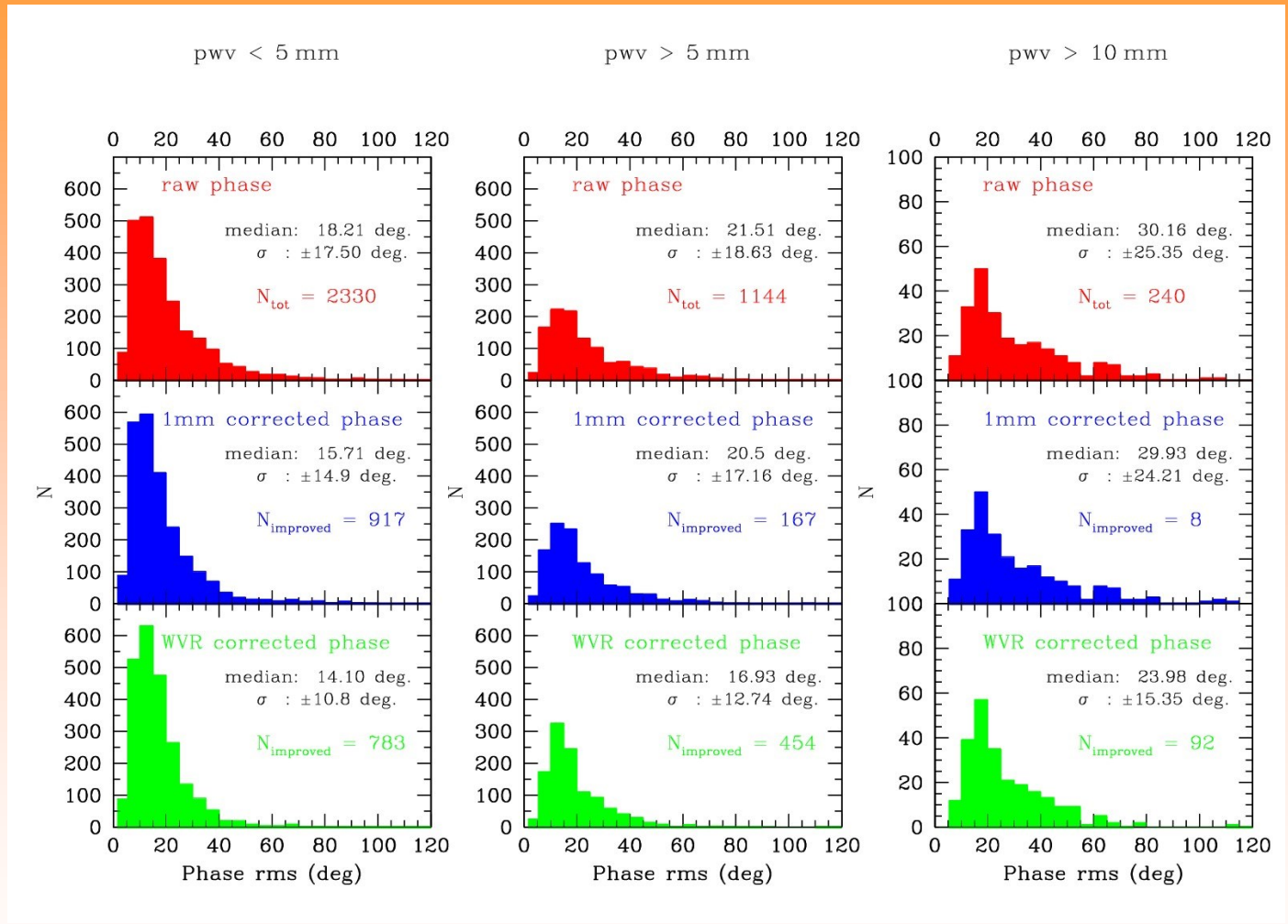

PdBI Histogram statistics on raw phase, 230 GHz corrected phase and WVR corrected phase show that the WVRs perform equivalent or better than the 230 GHz monitoring.

Now 8 antennas, but only 7 radiometers: the proxy correction

Copy the WVR data from the closest antenna.
Works if the phases are not too noisy.

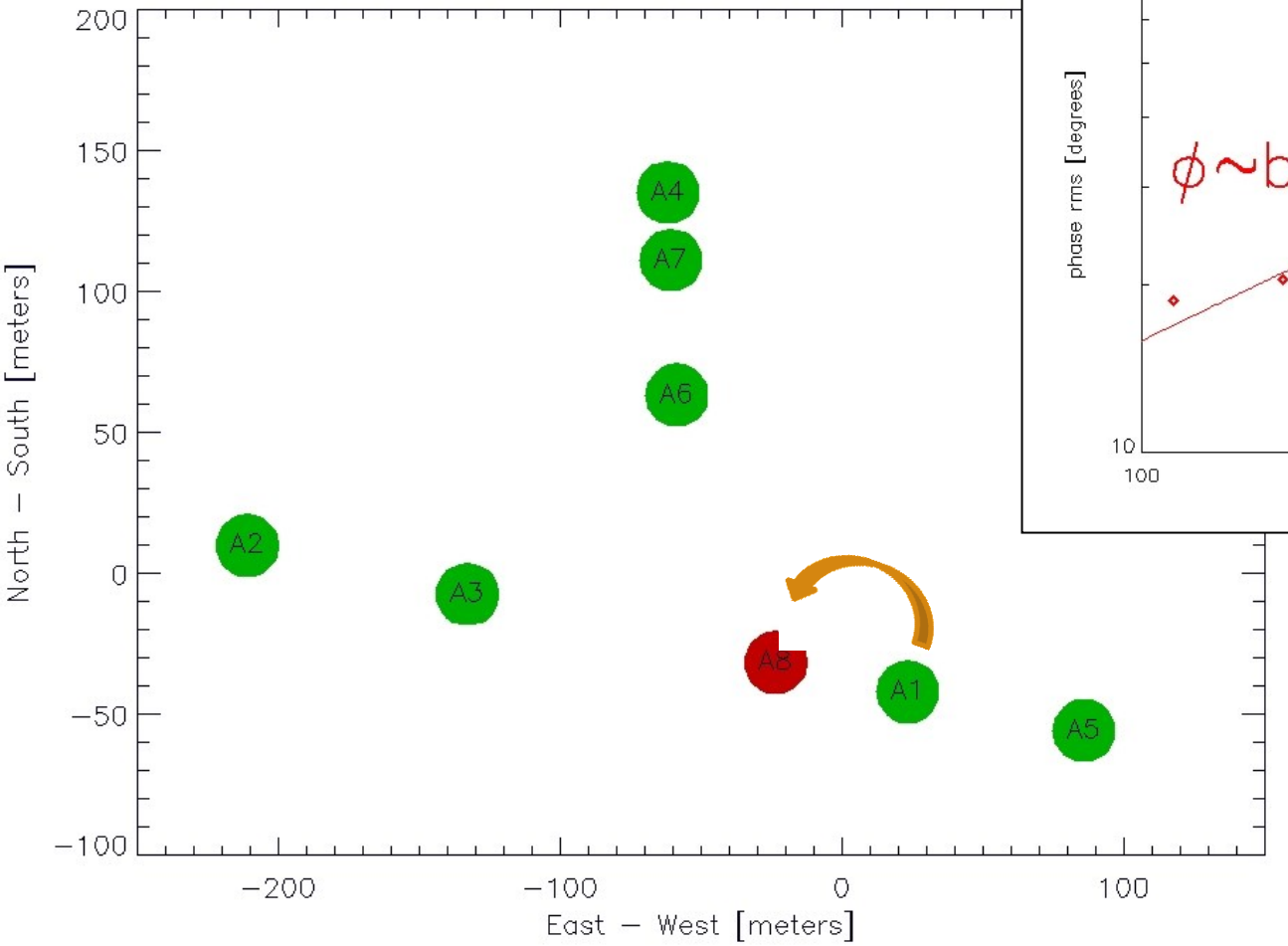

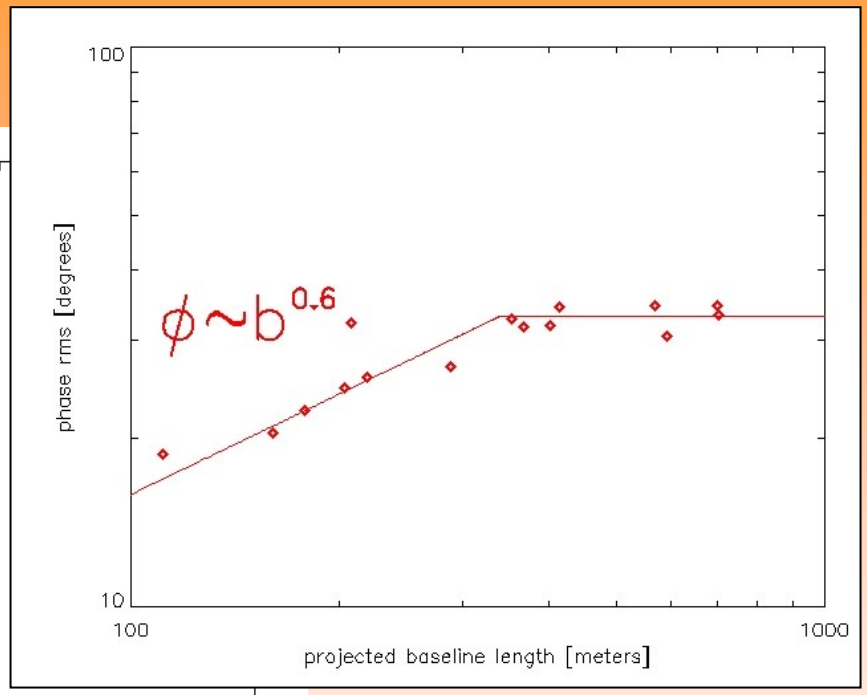

Preliminary solution.
A dedicated WVR is always better .

Now 8 antennas, but only 7 radiometers: the proxy correction

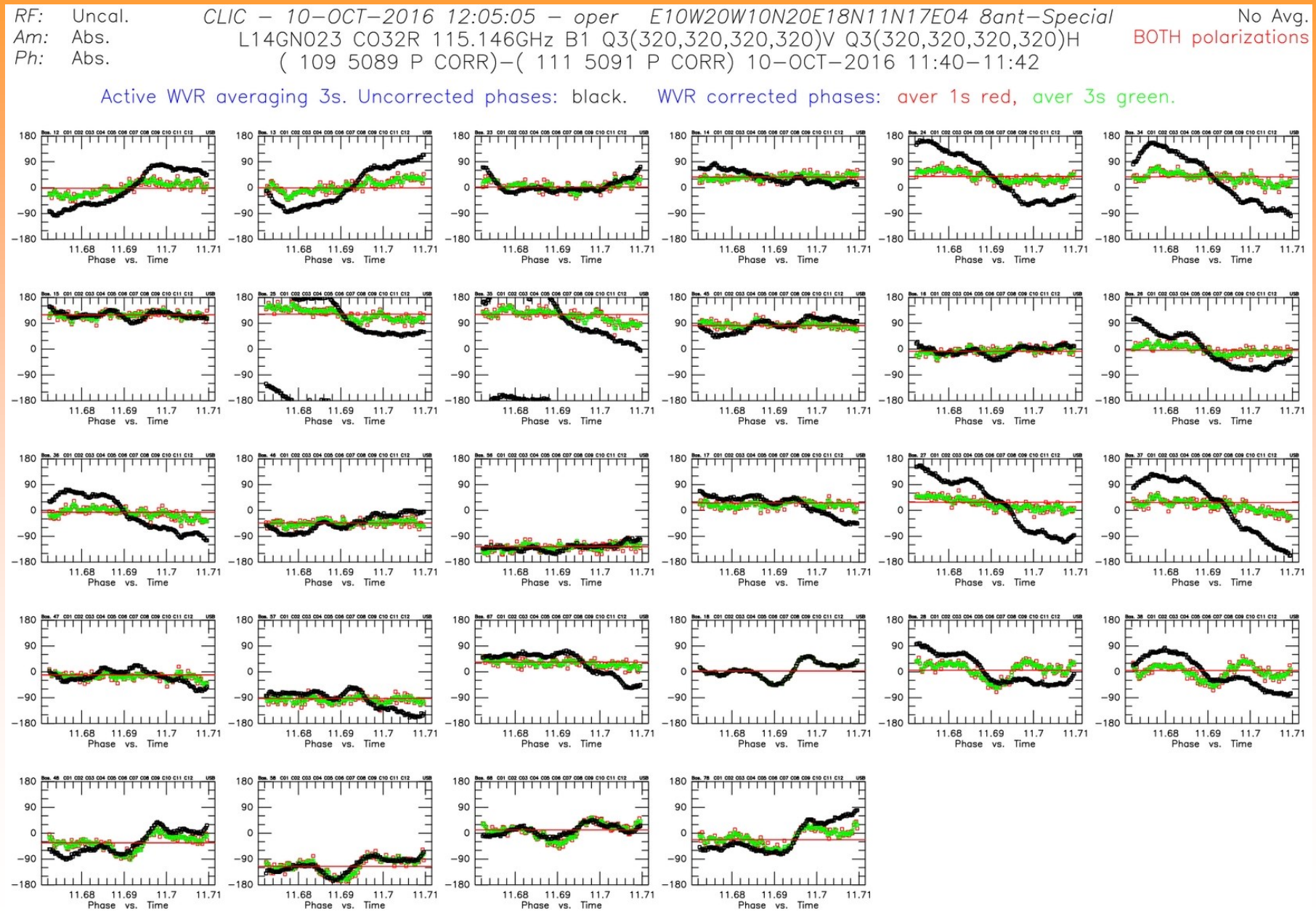

Appearance in the Bure data reduction

A simple mouse button starts procedures that are worth hours of command line typing. The following parts are related to phase correction:

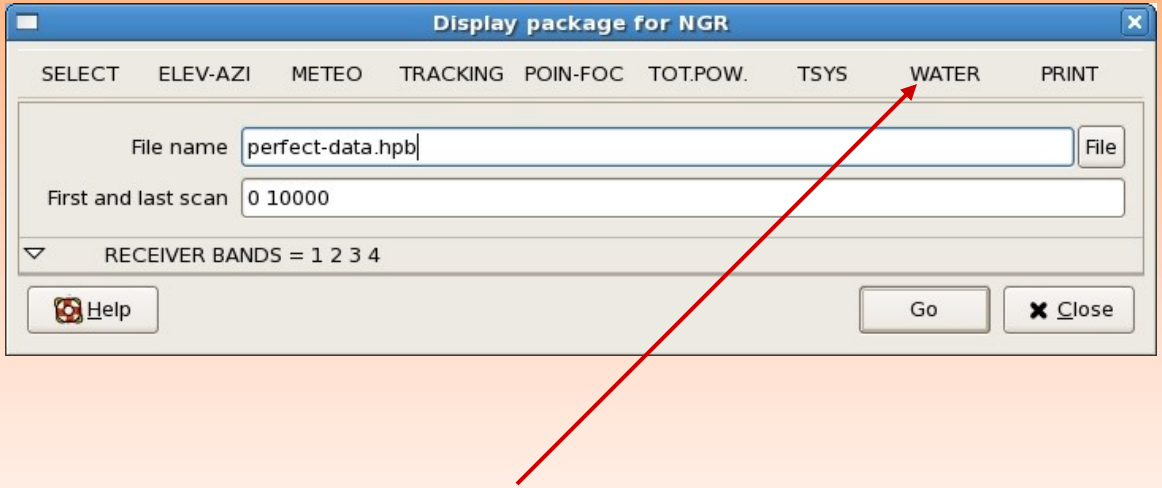

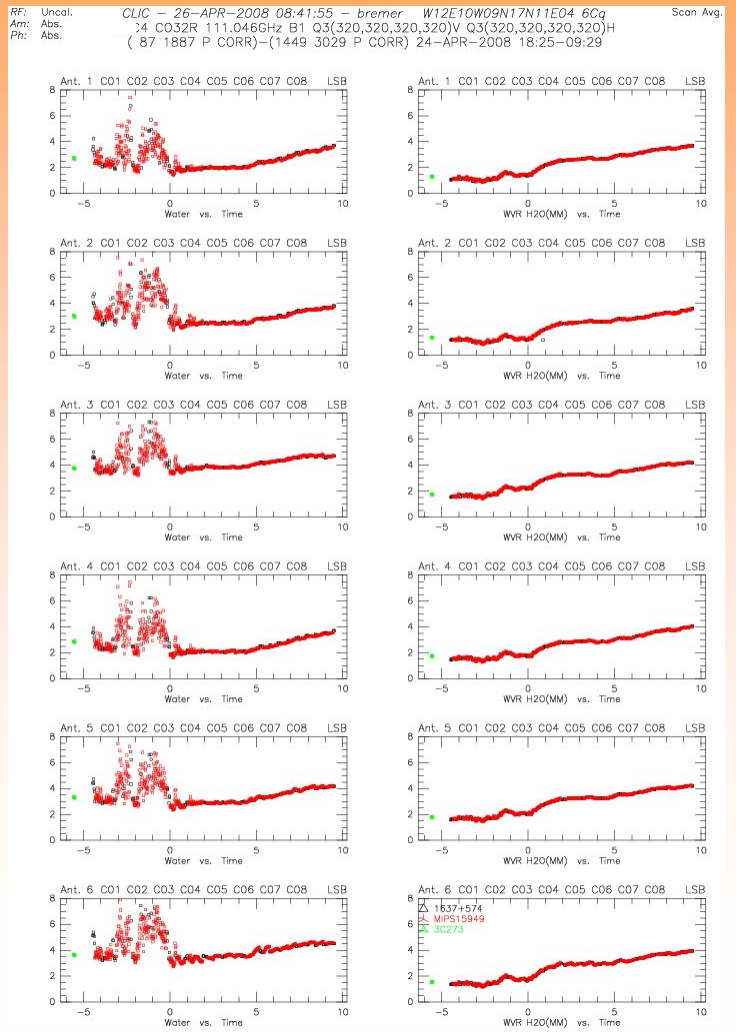

Comparison of the astronomical receiver and radiometer-derived precipitable atmospheric water

Appearance in the Bure data reduction

The menus evolve with CLIC versions, and may change. Here the Oct-2012 menus.

Verify where the phase correction improves the amplitudes

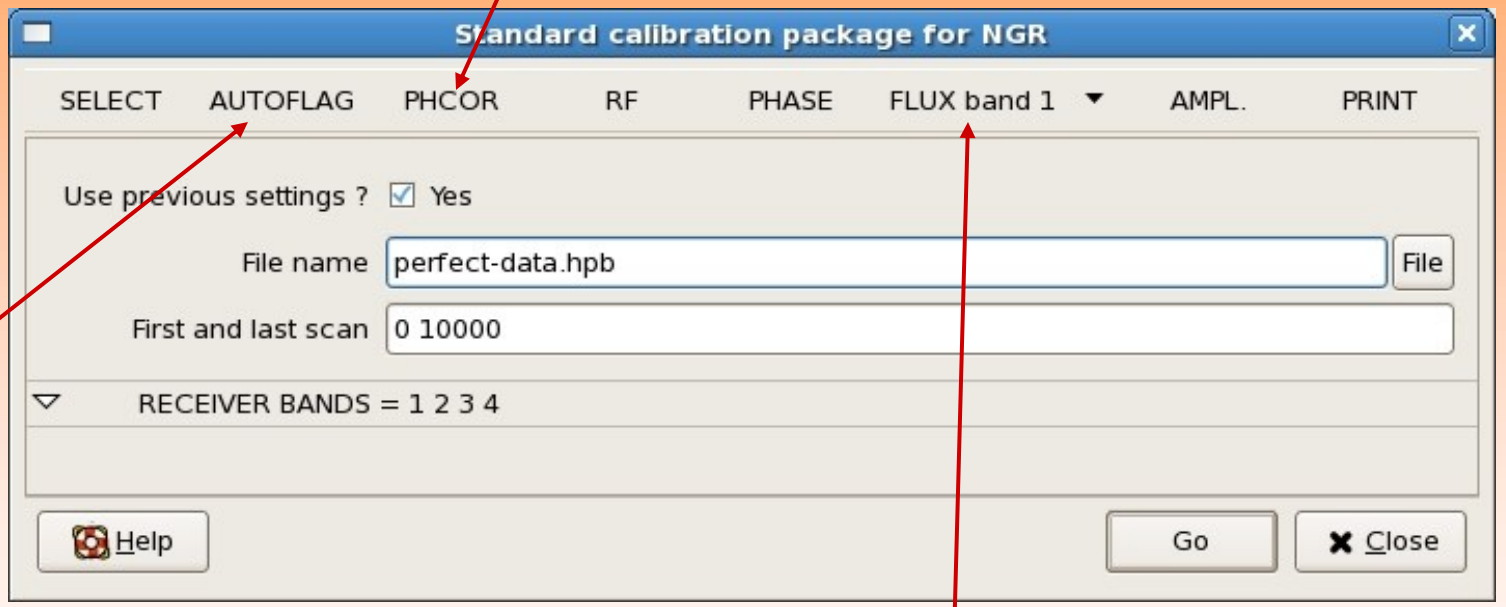

Contains an interference check

By default, the phase correction is switched ON.

Marks where the phase correction has been accepted

Useful checks

So far, interference has been detected from at least four satellites. In 2007, less than 0.5% of observations showed traces, but this number goes up.

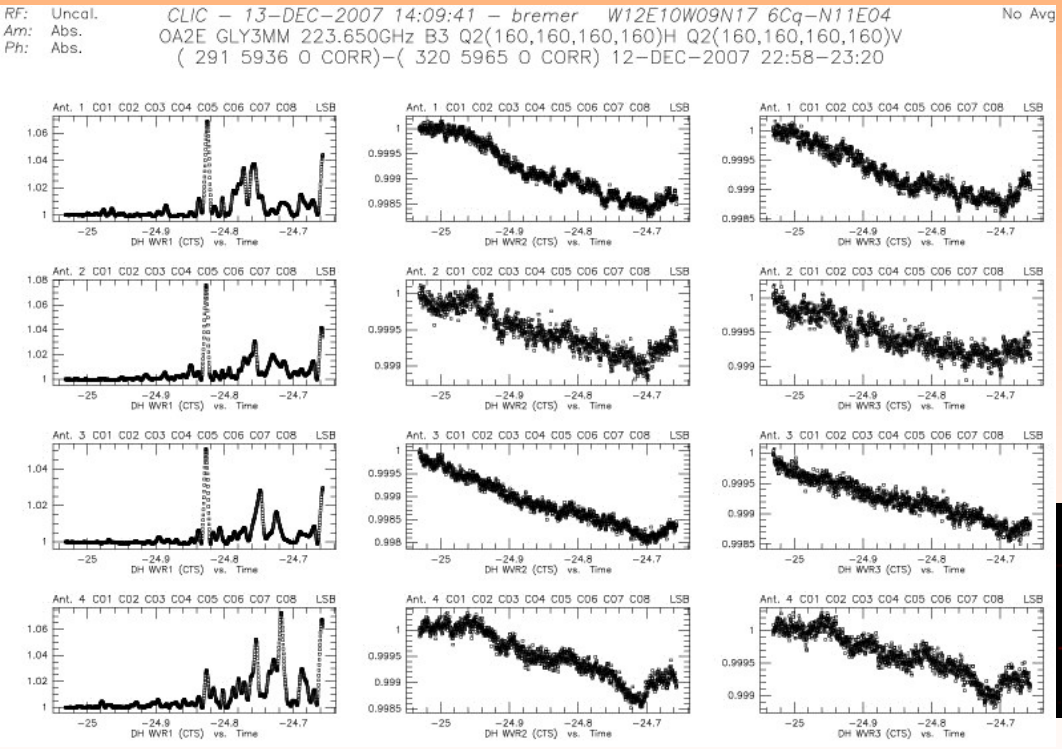

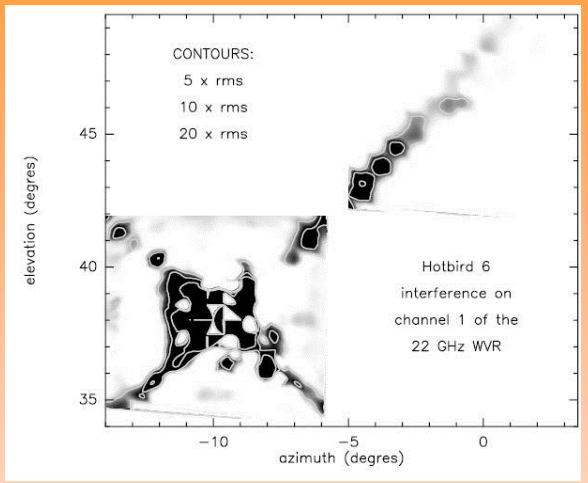

Strongest source:
Hotbird 6 (Alcatel Space) downlink

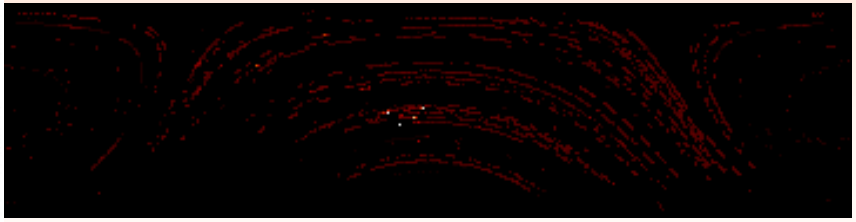

Scan based detection and flagging is possible by studying the following ratio:

$$\text{rms}\,[T_1 - T_2 \cdot \upsilon_1^2/\upsilon_2^2] \;/\; \text{rms}\,[T_2 - T_3 \cdot \upsilon_2^2/\upsilon_3^2]$$

Useful checks

The pipeline reduction plot shows information on the radiometers:

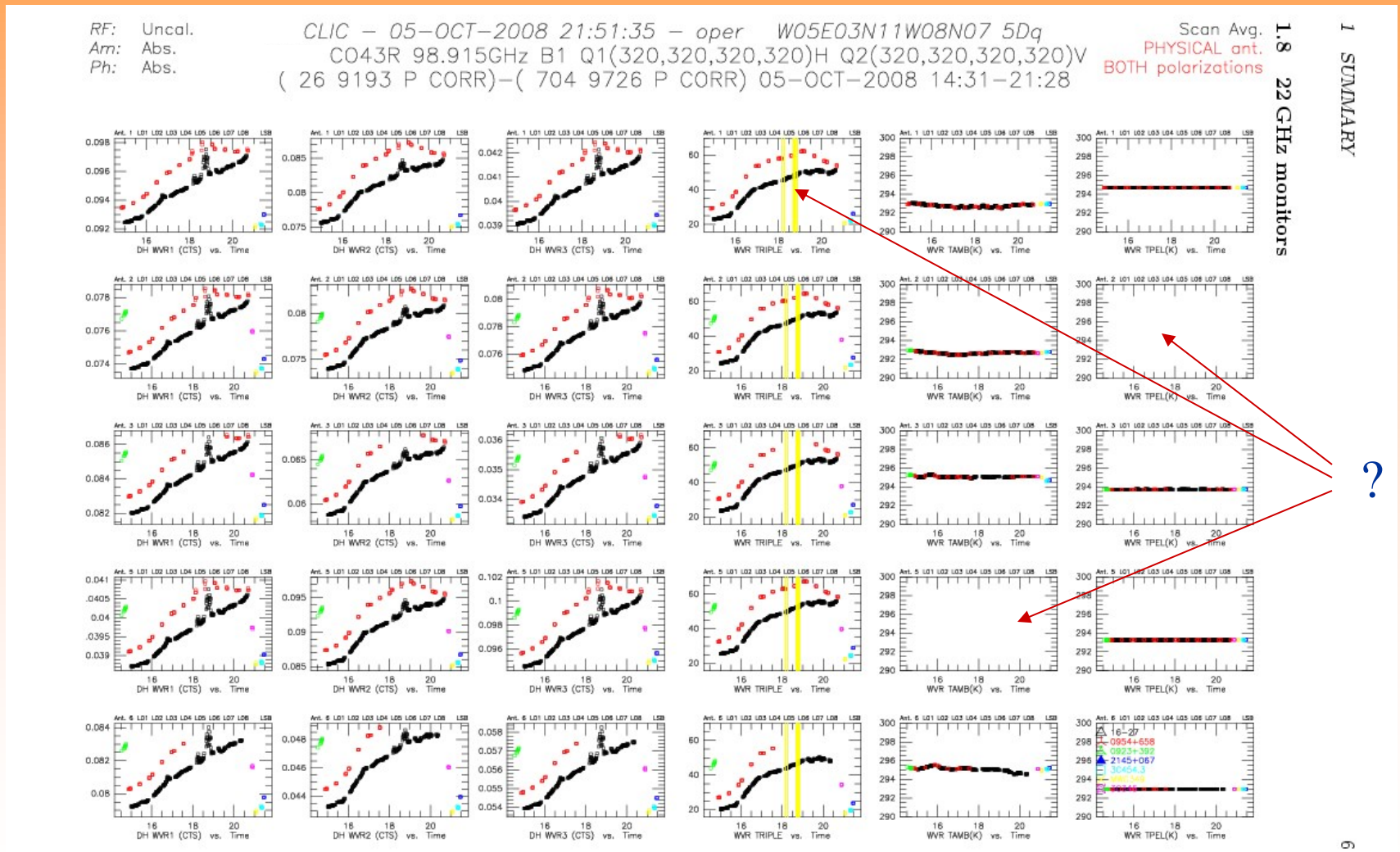

Fine tuning

- verify if there are spurious “interference” flags (can happen for some clouds)
- Check if the receiver cabin temperature does not oscillate by more than 1°C / hour
- check if a calibrator is not so weak that the amplitude improvement is not significant (that may flag the phase correction on the following source scans)
- in case of doubt, ask the local contact.

Fine tuning - some experimental maps

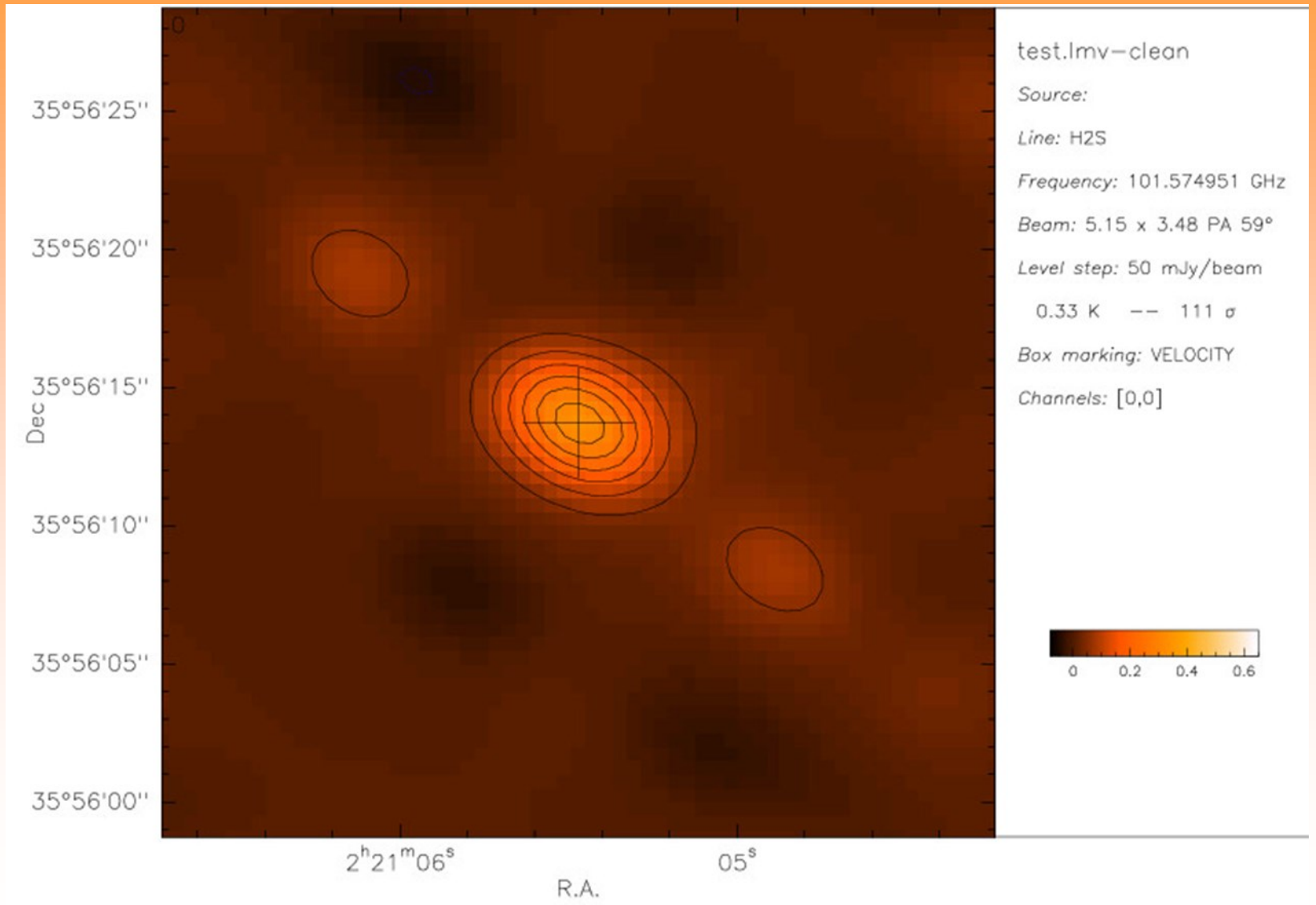

Fine tuning - some experimental maps

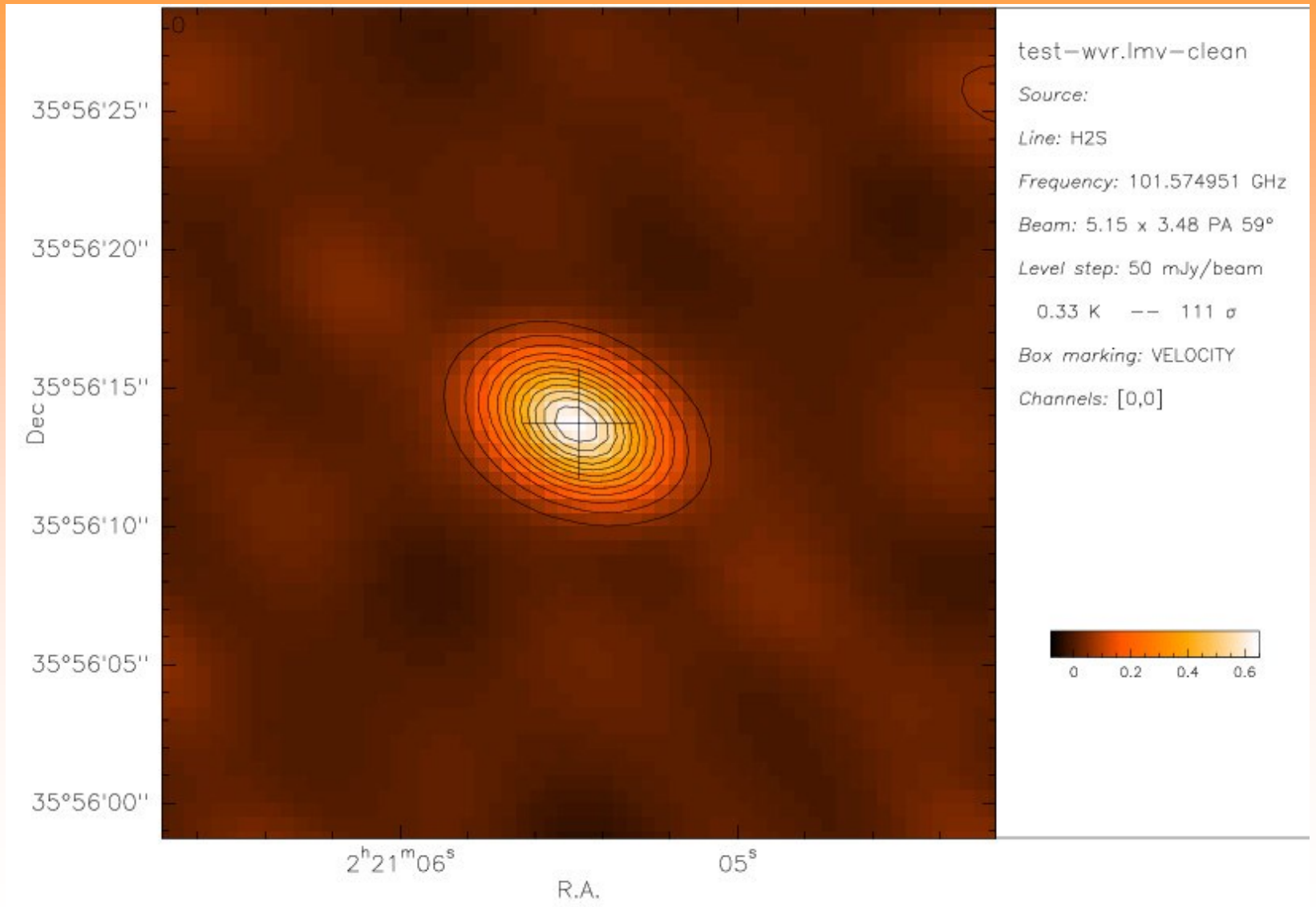

Outlook:

- **A new 22 GHz radiometer with 16 channels is under development.**
- **A new pipeline tool to extend the phase correction over 3 scans is in the testing phase (and looks promising).**

Thank you!